

**EFFECTS OF CLEAR WEATHER  
CONDITIONS ON SATELLITE AUDIO  
SIGNALS IN AKURE SOUTH WEST, NIGERIA.**

**By**

**ADENODI RAPHAEL ADEWALE**

**BSc (Ed) PHYSICS**

**(PHY/97/9931)**

**A thesis in the Department of Physics submitted to the  
School of Postgraduate Studies, in partial fulfillment of the  
requirements for the award of Master of Technology in  
Instrumentation and Measurement of the Federal University  
of Technology, Akure, Ondo State, Nigeria.**

**2005**

## CERTIFICATION

- (A) **BY THE STUDENT:** This work has not been presented elsewhere for the award of a degree, or any other purpose

**ADENODI, RAPHAEL ADEWALE**  
Candidate's Name

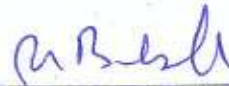


Signature

20/10/2005  
Date

- (B) **BY THE SUPERVISORS:** We certify that this work has been carried out by ADENODI, Raphael Adewale in the department of Physics of the Federal University of Technology, Akure.

**Dr. M. T. Babalola**  
B.Sc, M.Sc, Ph.D (Ibadan)  
Major Supervisor



Signature

28/11/05

Date

**Dr. M. O. Ajewole**  
B.Sc, M.Sc, (Ilorin), Ph.D (Akure)  
Co-Supervisor




Signature

28-11-05

Date

**Prof (Mrs) I. A. Fuwape**  
B.Sc, M.Sc, Ph.D (Ibadan)  
Head of Department



Signature

28-11-05

Date

## DEDICATION

This work is dedicated to the glory of God Almighty.



## ACKNOWLEDGEMENT

To God Almighty, the ever-present help in all troubles be glory and honour for the completion of this study. Words are inadequate to express my gratitude to my dear wife, Deborah, Omoyeni, for her all round support. May God bless you more. Erioluwa, my dear daughter and Shalom, my dear son, I appreciate you.

My sincere thanks to my able supervisors, Dr M.T Babalola and Dr Dare Ajewole for their encouragement and support. They contributed immensely towards the success of the project. I cannot thank you enough for your contributions. May God bless you.

I also appreciate the support of my parents Mr. and Mrs. Olorunfemi Adenodi, Late Elder and Mrs. Olomi Komolafe for their moral and spiritual support. My brothers and sisters: Anthony, Henry, Engr. Ayo, Dr. Johnson, Veronica, Adesani, Leke, Sola, Akinmade Taye and Sanmi for their love.

I wish to acknowledge the assistance of my church elders: Pastor and Mrs. Joshua Odeyemi, Pastor and Mrs. Ogunjemiluyi, Dr. and Mrs. Olumekun, Pastor and Mrs Famodimu and all members of Reconciliation House, Akure. Evang. and Mrs. Ife Akinyosoye, Mr. And Mrs. Emmanuel Okogbue, Ven (Dr.) and Mrs C.T. Omotunde and all members of Ecousa are appreciated for their encouragement. Last but not the least, my reserved gratitude to Dr. and Mrs. Olumide, Eng. Gbenga Adu, Eng. Dapo Ogunsanya, the management and staff of Adams communications, Akure, for the provision of mould and all Staff of Physics Department, (FUTA) and St Helen's Unity Secondary School, Ondo. God bless you all.

## TABLE OF CONTENTS

Title page	i
Dedication	ii
Acknowledgement	iii
Certification	iv
Table of contents	v
List of figures	viii
List of tables	viii
Abstract	ix
<b>Chapter 1</b>	
1.0 Introduction	1
1.1 Communication system analysis	1
1.2 Path loss capability	2
1.3 Motivation	3
1.4 Research Methodology	3
1.5 Order of Thesis	4
1.6 Research Objective	5
<b>Chapter 2</b>	
2.0 Literature review	7
2.1 The atmosphere	7
2.2 Free space path loss	8
2.3 Satellite distance	9
2.4 Elevation angle	11
2.5 Azimuth angle	13
2.6 Anomalous propagation	14
2.7 Tropospheric Refraction	15
2.8 Basic Physics of ionosphere	16
2.9 The ionosphere	17
2.10 Radiative heating and ionization mechanism	18
2.11 Properties of ionized medium	20

2.12 Magneto-ionic theory and Appleton-Hartree equation	22
2.13 Faraday rotation-----	25
2.14 Polarization loss factor-----	26
2.15 Cross polarization due to rain-----	27
2.16 Dielectric properties of water-----	28
2.17 Raindrop shapes -----	29
2.18 Canting angle of raindrops-----	30
2.19 Raindrop fall velocity-----	30
2.20 Raindrop size distribution model -----	32
2.21 Slant path in rain region-----	34
2.22 Cross polarization isolation and discrimination-----	35

### Chapter 3

3.0 Earth station-----	39
3.1 Microwave antenna-----	40
3.2 Antenna size-----	40
3.2.1 Illumination efficiency-----	42
3.2.2 Spillover efficiency-----	42
3.2.3 Surface finish efficiency-----	42
3.2.4 Dish obstruction-----	44
3.3 Methods of construction-----	45
3.3.1 Moulding-----	45
3.4 Focal length to diameter ratio ( $F/D_A$ )-----	47
3.5 LNB and LNBF-----	50
3.6 Dish feed system-----	51
3.7 Circular feed-----	52
3.8 Phase centre of feed-----	54
3.9 Polariser-----	54
3.9.1 Vertical /Horizontal switching type-----	55
3.9.2 Ferromagnetic polariser-----	55
3.9.3 Mechanical motor driven types-----	55
3.10 Figure of merit -----	56

3.11 Carrier to noise ratio -----	57
3.12 Antenna noise temperature -----	58
<b>Chapter 4</b>	
4.0 Measurements and calculations -----	59
4.1 The signal path length -----	66
4.2 Ionospheric path length -----	69
4.3 Absorption index -----	69
4.4 Polarization mismatch loss -----	72
4.5 Cross polarization determination -----	72
4.6 Overall loss -----	75
4.7 Figure of merit -----	75
<b>Chapter 5</b>	
5.0 Discussion and recommendation -----	78
5.1 Discussion of Results -----	78
5.2 Recommendation -----	80
References -----	81



## LIST OF FIGURES

- Fig 2.1 Atmospheric mean temperature profile
- Fig 2.2 Satellite-earth geometry
- Fig 2.3 Geometry of elevation angle
- Fig 2.4 Variation of electron density against height
- Fig 2.5 Raindrop shape (a) oblate spheroidal shape  
(b) prolate spheroidal shape
- Fig 2.6 A model of raindrop canting angle
- Fig 2.7 Schematic representation of earth-space path
- Fig 2.8 Schematic representation of cross polarization isolation and cross polarization discrimination
- Fig 3.1 Feed pattern showing illumination and spillover losses
- Fig 3.2 A simple waveguide transition of circular horn feed
- Fig 4.1 (a-p) Audio waveform

## LIST OF TABLES

- Table 4.1 Audio signal in voltage and video signal in gigahertz
- Table 4.2 Equivalent dB values and polarizations
- Table 4.3 Elevation angle and free space loss for frequency 22KHz
- Table 4.4 Ionospheric absorption of ordinary and extraordinary waves of frequency 22KHz
- Table 4.5 Total mismatch loss
- Table 4.6 Cross polarization discrimination
- Table 4.7 C/No and path loss capability.

## ABSTRACT

This project was carried out to analyse the performance of Satellite Television Receive Only (TVRO) communication systems in terms of the propagation loss in the C-band (6/4 GHz) frequencies. A 3.0m parabolic dish was constructed by the method of moulding using glass fibre. This dish was used to receive audio signals from some satellites and the field strength measured by a 40MHz oscilloscope. The results show that the noise temperature of the parabolic dish was reasonably low thus resulting in low system noise temperature, high carrier to noise ratio and high figure of merit for the TVRO. The atmospheric losses in channels on satellites in the eastern hemisphere are higher than those in satellites located in the western hemisphere. This is due to the low elevation angle of satellites in the east which resulted in the signals travelling longer path lengths in this hemisphere. There was no appreciable loss associated with the receiving system, rather the system improved the level of the weak signal received thus resulting in quality intelligent output by the indoor receiver-monitor combination.

## **CHAPTER ONE**

### **1.0 INTRODUCTION**

1.0

A basic communication system consists of a transmitter and a receiver, each with its associated antenna, the two being separated by the path to be covered. In order to generate an intelligible output, the receiver requires a certain minimum signal called the static threshold which is to be collected by its antenna and presented to its input socket. Radio wave communication between any particular transmitter and receiver depends primarily on the transmitter power, sensitivity of the receiver and the loss associated with the path between them.

Usually, the transmitter generates a much stronger signal than the minimum required by the receiver, hence a large loss of signal may be tolerated. For many path of interest, the actual path loss may be larger and communication may therefore become impossible. An added complication is that, the variation in path loss over a given path for a period of time can be large. If communication is to be maintained for a high proportion of time, a relatively powerful equipment will be required in order to cope with poor propagation conditions.

### **1.1 COMMUNICATION SYSTEM ANALYSIS**

It has already been stated that the possibility of radio wave communication between a transmitter and a receiver depends on the power of the transmitter, the sensitivity of the receiver and the path length between them, among other factors. The objective of communication system analysis is to quantify these factors so that the performance of a communication link can be predicted. The

result of the system analysis can be used to determine the initial design of equipment for a link, to determine the suitability of existing equipment to communicate over a given path and, if the way in which the path loss varied with time is known then the percentage of total time that communication is practicable can be predicted. In the latter case, the analysis will also indicate by how much the potency of the equipment must be increased to produce acceptable level of communication.

## 1.2 PATH LOSS CAPABILITY

The path loss capability is the maximum path loss that a particular equipment can tolerate and is defined, as the ratio of the power generated by the transmitter to the minimum required by the receiver. If the actual path loss is greater than the path loss capability then communication is not possible. Mathematically, the path loss capability is

$$Plc \text{ (Watts)} = \frac{\text{Effective power of transmitter}}{\text{Minimum power to operate receiver}} \quad (1.1)$$

It can also be written as

$$Plc \text{ (dB)} = eirp - ers \quad (1.2)$$

where eirp and ers are figures of merit of the transmitter and receiver respectively. The figure of merit of a transmitter is the effective isotropic radiated power (eirp) which is defined as the power required to be radiated from an isotropic source to produce the same signal at the receiver input as the actual transmitter – receiver combination. The minimum power a receiving antenna

must collect in order that the receiver can generate an intelligible output is called the effective receiver sensitivity (ers).

### 1.3 MOTIVATION

Signals from space stations are received at earth stations after passing through a distance of about 35,000km in the atmosphere. The signal strength of the electromagnetic wave reduces as it propagates through the atmosphere. It is therefore necessary to quantitatively determine the loss due to atmospheric influence in terms of free space path loss and ionospheric absorption, and the loss due to system inadequacy in terms of dish surface imperfection and polarization mismatch at the receiving probe. When an earth station is aligned with two or more space stations, the elevation angles of the space stations are not the same except the satellites are located in the same longitudes. The dependence of the signal loss on elevation angle shall also be considered in this study.

### 1.4 RESEARCH METHODOLOGY

A 3.0m parabolic dish was constructed using a concrete mould. After washing the mould surface with a mixture of water and detergent and allowing dry, an aluminum foil was laid on the mould followed by layers of fiberglass. Resin solution (phenol-formaldehyde) was now spread on it. Then the parabolic dish metal frame was placed on the mould, followed by other layers of fiberglass before the addition of resin to ensure firm grip between the fiber, aluminum foil

and the metal frame. After five hours the dish was sufficiently dry and ready for use. The parabolic dish was used to received signals from satellites, some located in the east and others in the west. A 40MHz oscilloscope measured the levels of the audio signals received, at frequencies the C-Band (6/4GHz). The receiver parameters and various losses were computed as well as the figure of merit of the space transmitters.

## 1.5 ORGANISATION OF THESIS

This study deals with the effects of clear weather condition on satellite audio signals received at longitude  $5.2^{\circ}\text{E}$  and latitude  $7.28^{\circ}\text{N}$ . The thesis consists of five different chapters and each chapter deals with a distinct aspect of the study. The introduction chapter, which is the first chapter, deals with the analysis of communication system. It is mentioned in this chapter that the possibility of communication between a transmitter and a receiver depends on the transmitter power, the sensitivity of the receiver and the loss associated with the propagation path between them. Chapter two is centered on the description of the propagation path and the losses incurred during propagation. The lower atmosphere is dominated by the overwhelming influence of neutral air unlike the upper atmosphere where electron and charges are sufficiently numerous. The propagation losses are in the form of free space loss and ionospheric absorption. The determination of the antenna efficiency and gain, the noise temperature of the TVRO and the construction of parabolic dish by the method of moulding were explain in chapter three while chapter four deals with the quantitative

determination of the atmospheric and system induced losses, the effective receiver sensitivity of the earth station and the effective isotropic radiated power of the space stations. Finally chapter five contains the discussion of results and recommendation.

## 1.6

### RESEARCH OBJECTIVE

A 3.0 m parabolic dish antenna was constructed using fibreglass. The dish antenna was used to receive both video and the audio frequency components of linearly polarized signals from some satellites at frequencies in the C- band (6/4GHz). The received audio signal was measured in voltage and then converted to its decibel equivalent. This research is to consider and estimate the loss in energy of radiowave propagating through the atmosphere in the absence of meteorological formation. The following parameters were then calculated so as to determine the degradation of the received audio signal due to system and atmospheric induced losses.

- The free space path loss
- The level of signal absorption in the ionosphere
- The degree of rotation of the plane of polarization of the wave
- The polarization loss factor
- Efficiency of the parabolic dish
- Figures of merit of transmitter and the receiver
- The carrier to noise ratio of the television receive only (TVRO).
- The path loss capability.

The video component of the signal was not investigated because of the inavailability of a channel/spectrum analyzer that could measure input signal in the GHz range.

## CHAPTER 2

### 2.0

## LITERATURE REVIEW

### 2.1

## THE ATMOSPHERE

The success of any communication system depends on the influence of the propagation medium. The parts of the atmosphere are best described in terms of the vertical temperature profile. They include the troposphere (0 - 11km approx.) where the temperature decreases upward from its ground level value. The stratosphere (11-50km) is a region with high ozone concentration and temperature increases with altitude. The mesosphere (50 – 85km) is a region of higher temperature heated by the absorption of solar ultraviolet radiation and by a small amount of ozone. Temperature decreases with altitude in this region. The thermosphere is above 85km and is the region that is strongly heated by solar extreme ultraviolet radiation and X-ray that dissociates and ionizes the atmospheric gases, and thus creates a fairly large portion of the ionosphere. The ionization of gases and the concentration of free electrons are very intense in this region called the ionosphere. Above the ionosphere lies the exosphere (above 600km), the air in this region is too thin to be considered as a gas. The individual atoms move freely in orbits (Hall and Barclay, 1991).

The atmosphere is a mechanical mixture of gases, not a chemical compound. Nitrogen, oxygen, argon and carbon dioxide account for about 99.9% of the air by volume. Rocket observations showed that these gases are mixed in remarkable constant proportion up to about 100km. Neon, helium and methane have very negligible percentage composition. In addition to these gases, water

vapour and ozone are much more variable in their occurrence in time and space. They are vital atmospheric constituents since both absorb solar and terrestrial radiation. The heat budget and vertical temperature structure of the atmosphere are considerably affected by the distribution of these two gases. Figure 2.1 shows atmospheric mean temperature profile. There is also significant quantity of aerosols in the atmosphere. These are suspended particles of dust, organic matter and smoke. They come from both natural and man-made sources (Roger and Richard, 1982).

Atmospheric effects on radio wave propagation include attenuation, depolarization, cross polarization, scattering, absorption, refraction and reflection to mention a few. Each of these effects reduce the signal level intercepted by the receiving antenna. This research is to consider and estimate the loss in energy of radiowave propagating through the atmosphere in the absence of meteorological formations.

## 2.2 FREE SPACE PATH LOSS

Microwave propagation from the transmitting earth station to the space station and from there to the receiving earth station is through line of sight mode. As there will be no effect due to obstruction in the atmosphere. The radiation intensity decreases as the square of the distance from the transmitting antenna. In other words, the path loss increases as the square of the distance between the transmitting and the receiving antennae due to the fact that radiation emitted

spreads out equally in both the horizontal and vertical planes and both are perpendicular to the direction of propagation.

According to Timothy and Charles (1986), the actual path loss is

$$L_A = 20 \log \left( \frac{4\pi r}{\lambda} \right) \quad (2.1)$$

where  $r$  and  $\lambda$  are distance and wavelength in metres. However some other mathematical relations specified by Radio Society of Great Britain (1994) can be used, which are

$$L_A = 32.45 + 20 \log(f) + 20 \log(r) \quad (2.2)$$

where  $f$  is frequency in megahertz and  $r$  is distance in kilometers.

$$\text{Also } L_A = 92.45 + 20 \log(f) + 20 \log(r) \quad (2.3)$$

$f$  is frequency in gigahertz and  $r$  is distance in kilometers.

### 2.3 SATELLITE DISTANCE

In figure 2.2, S is the satellite, S' is earth station and T is the subsatellite point, that is, where the line joining the satellite and earth's center passes through on the earth's surface. Considering triangle OS'S, the distance  $r$  between the satellite S and earth station S' is given as (UNESCO, 1996)

$$r^2 = D_L^2 + R^2 - 2D_L R \cos \beta \quad (2.4)$$

where  $D_L$  is the distance between the satellite and earth's center and  $R$  is radius of earth,  $\beta$  is angle subtended at the earth's centre by  $R$  and  $D_L$ .

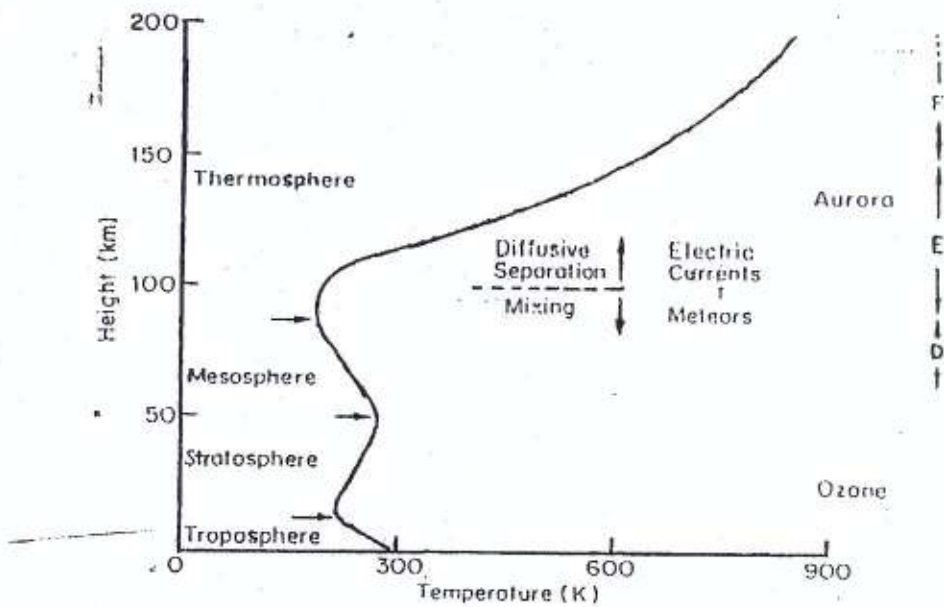


Fig 2.1 Atmospheric mean temperature profile

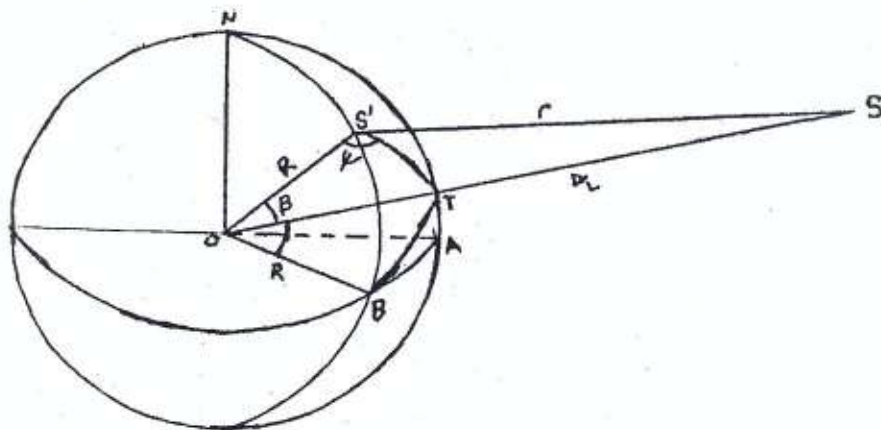


Fig 2.2 Satellite – earth geometry

According to Timothy and Charles (1986) angle  $\beta$ , is given by

$$\cos \beta = \cos \alpha_e \cos \alpha_s \cos(\phi_s - \phi_e) + \sin \alpha_e \sin \alpha_s \quad (2.5a)$$

where  $\phi_s$  and  $\phi_e$  are subsatellite and site longitudes, and  $\alpha_s$  and  $\alpha_e$  are subsatellite and site latitudes. Latitude of subsatellite,  $\alpha_s = 0$  and  $\phi_s - \phi_e = \Delta\phi$ , the difference between the longitude of site and subsatellite.

Therefore

$$r^2 = D_L^2 + R^2 - 2D_L R \cos \Delta\phi \cos \alpha_e \quad (2.5b)$$

## 2.4 ELEVATION ANGLE

The coordinates to which an earth station antenna must be pointed to communicate with a satellite are called the look angles. The angles are commonly specified as elevation angle  $\theta$  (fig.2.3) and azimuth angle, Az

The elevation angle is the angle between the local horizon and the satellite, measured in the plane containing the earth station, the satellite and the earth's centre. (Maral and Bousquet, 1998)

By the sine rule 
$$\frac{r}{\sin \beta} = \frac{D_L}{\sin \psi} \quad (2.6)$$

The local horizon is usually perpendicular to the radius of the earth R at the station. Therefore,  $\psi = 90^\circ + \theta$

$$\theta = \arccos \left( \frac{D_L \sin \beta}{r} \right) \quad (2.7)$$

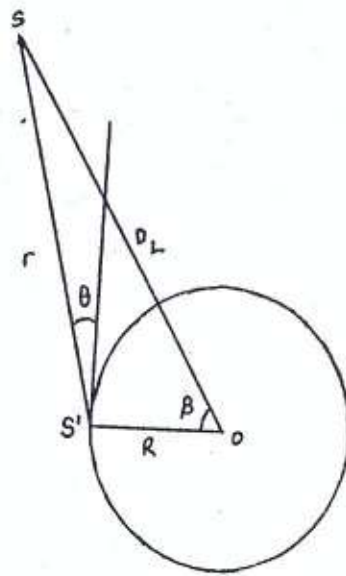


Fig. 2.3 The geometry of elevation angle

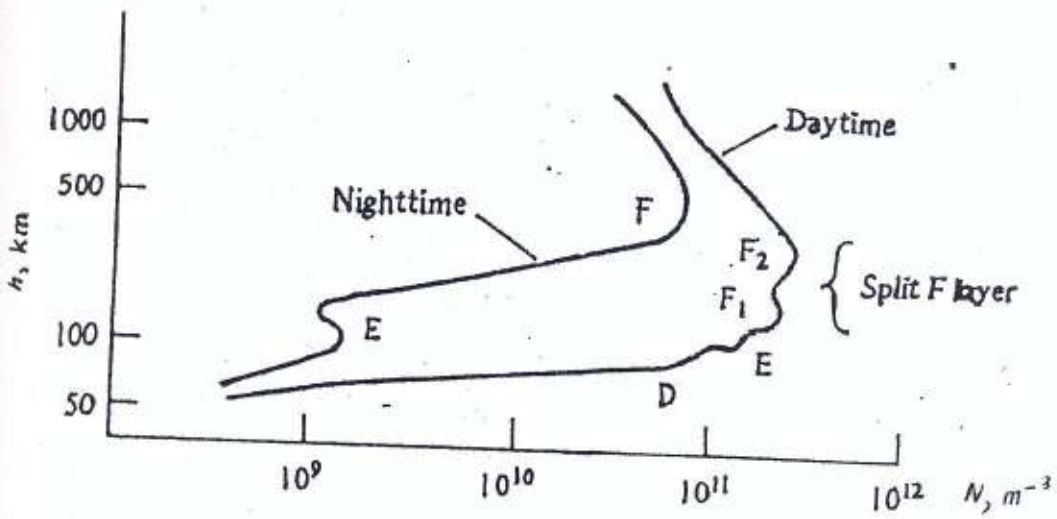


Fig. 2.4 Variation of electron density against height

For a satellite to be visible at an earth station, its elevation angle must be above some minimum value, at least zero. A positive angle requires that

$$D_L \geq \frac{R}{\cos \beta} \quad (2.8)$$

The value of angular separation,  $\beta$ , between the site and subsatellite point is limited by

$$\beta \leq \arccos \left( \frac{R}{D_L} \right) \quad (2.9)$$

For a geostationary satellite,  $\beta$  is less or equal to  $81.3^\circ$  (Pratt and Bostian, 1986). A smaller angular separation is desirable so as to avoid propagation problem associated with extreme low elevation angle. For this study  $\beta$  will be taken to be  $81.3^\circ$  and therefore the value of  $D_L = 42.17 \times 10^6 \text{ m}$ .

## 2.5

### AZIMUTH ANGLE

The azimuth angle, Az, is the angle measured in a horizontal plane of the location between the direction of geometrical north and the intersection of the plane containing the satellite and the centre of the earth (Maral and Bousquet, 1998). The angle varies between  $0^\circ$  and  $360^\circ$  as a function of the relative position of the satellite and the earth station. According to Maral and Bousquet (1998), the azimuth angle, Az, depends on the location of the earth station with respect to subsatellite point. Therefore the azimuth angle is deduced as follows;

subsatellite point southwest of earth station,  $Az = 180 + \alpha$

subsatellite point southeast of earth station,  $Az = 180 - \alpha$

subsatellite point northwest of earth station,  $Az = 360 - \alpha$

subsatellite point northeast of earth station,  $Az = \alpha$

$$\text{where } \alpha = \arctan \left( \frac{\tan \Delta \phi}{\sin \alpha_e} \right) \quad (2.10)$$

## 2.6 ANOMALOUS PROPAGATION

Under normal propagation condition, radiation intensity reduces as the square of the distance from the transmitter because the radiation spreads out both in vertical and horizontal planes. Anomalous propagation is a condition in which the spreading out takes place majorly in one of the plane and confined in the other plane. This confining process leads to a reduction in the path loss. The path loss simply increases with distance and not with the square of the distance (RSGB, 1994).

$$\text{Therefore path loss} = 10 \log(1.757 \times 10^{-15} r f^2) \quad (2.11a)$$

for frequency in hertz.

$$L_A = 32.45 + 20 \log(f) + 10 \log(r) \quad (2.11b)$$

for frequency in megahertz, and for frequency in gigahertz

$$L_A = 92.45 + 20 \log(f) + 10 \log(r) \quad (2.11c)$$

In most cases, the radiation is confined in the vertical plane. The difference in path loss between anomalous and normal propagation conditions makes anomalous condition desirable. Under anomalous propagation, actual path loss will never be greater than path loss capability of the equipment.

## 2.7 TROPOSPHERIC REFRACTION

Electromagnetic waves propagating through the troposphere are refracted due to the variations in the radio refractive index,  $n$ . The variations in the refractive index are caused by variations in atmospheric pressure,  $P$ , air temperature,  $T$  and water vapour pressure,  $e$ . Refractivity  $N$  is related to refractive index by (RSGB, 1994; Hall and Barclay, 1991)

$$N = (n - 1)10^6 \quad (2.12)$$

Refractivity is related to atmospheric pressure  $P$ , air temperature  $T$  and water vapour pressure  $e$  by (Smith and Weintraub, 1953)

$$N = \frac{77.6P}{T} + \frac{3.73 \times 10^5 e}{T^2} \quad (2.13)$$

The atmospheric pressure, air temperature and water vapour all decrease with increasing height. The first term on the right-hand side of equation (2.13) corresponds approximately to the optical value (dry term) while the second term accounts for the presence of water vapour (wet term) in the atmosphere. The refraction caused by the troposphere is significant at very small elevation angles and it may lead to loss of radiation in part or wholly missing the receiving antenna. If a significant amount of the radiation misses the receiving antenna, then the overall gain will suffer. If the axis of oncoming radiation misses the

receiving antenna boresight by  $\Phi$  , then the depointing loss incurred will be (Maral and Bousquet, 1998)

$$L_r = 12 \left( \frac{\Phi}{\Phi_{3dB}} \right)^2 \quad (2.14)$$

where  $\Phi_{3dB}$  is the 3dB beam width

## 2.8 BASIC PHYSICS OF IONOSPHERE

The ionosphere is identified as the part of the upper atmosphere where electrons are sufficiently numerous and these charges influence the propagation of radio waves. The behaviour of ions and electrons in the ionosphere is largely governed by the earth's magnetic field. The most important ionospheric parameter is the electron density  $N$  otherwise known as electron concentration.

The vertical distribution of any particle or gas is mainly controlled by gravity, which balances the vertical pressure gradient as shown by the hydrostatic or barometric equation (Hall and Barclay, 1991)

$$-\frac{dP}{dh} = \rho g = Nmg \quad (2.15)$$

where  $P$  = pressure,  $\rho$  = density,  $N$  = concentration,  $m$  = particle mass and  $g$  = acceleration due to gravity. The equation may be combined with the perfect gas law

$$P = NkT = \frac{\rho RT}{M} \quad (2.16)$$

where  $k$  is Boltzmann's constant,  $R$  = gas constant,  $T$  is temperature in Kelvin and  $M$  is molecular mass in atomic units. The equation can be integrated to give the variation of pressure with height above a base level  $h_0$ .

$$P = P_0 \exp\left(\frac{h_0 - h}{H}\right) \quad (2.17)$$

where  $H$  is known as scale height of the gas and is given as

$$H = \frac{kT}{mg} = \frac{RT}{Mg} \quad (2.18)$$

## 2.9

## THE IONOSPHERE

The ionosphere is the part of the upper atmosphere in which free electrons are sufficiently numerous to influence the propagation of radio waves. For practical purpose, it may be taken to lie between heights of about 70 and 600km but these are not well defined limits. The overwhelming influence of the neutral air in the lower atmosphere do not allow the electrons and ion present there to have any significant effect on radio wave propagating through it.

Marconi discovered the ionosphere when he sent radio signals across the Atlantic in 1901. Afterwards, Kennelly and Heaviside suggested that free electric charges in the upper atmosphere could cause the reflection of radio wave. Ionospheric physics really began with the experiments of Appleton and Barnett, Breit and Tuve in 1924/1925 that measured the height of the conducting layer and revealed its stratified nature (Hall and Barcley, 1991).

The ionization in the upper atmosphere is of practical importance because of its role in radio communications. It is important scientifically because the charged particles are easier to detect experimentally than the neutral gas and thus act as useful tracers for studying the upper atmosphere. Despite its importance, the ion is one of the minor constituents of the upper atmosphere. The ionosphere is electrically neutral to a very high degree of approximation, as positive and negative particles are created and destroyed together.

## 2.10 RADIOACTIVE HEATING AND IONOIZATION MECHANISM

The layers of ionosphere are formed by ionization as a result of radiation absorbed by atmospheric components. The extent to which any radiation of wavelength,  $\lambda$ , penetrates depends on the photo-absorption cross-section,  $\sigma$ , of the atmospheric constituents present. Photo-absorption cross-section is a measure of the efficiency with which any molecule absorbs light energy. If radiation of intensity  $I_0$  transverses thin layers of the atmosphere of thickness  $dz$ , the decrease in intensity is given by Campbell (1997) as

$$-dI = I_0 N \sigma dz \quad (2.19)$$

where  $N$  is the concentration per cubic metre of the absorber. If this is integrated over a slab of thickness  $Z$ , it yields

$$I = I_0 \exp(-N\sigma dz) \quad (2.20)$$

called the Beer-Lambert expression. For a homogeneous medium, the depth to which the radiation penetrates before its intensity become attenuated by a factor of  $\frac{1}{e}$  is the optical depth, which is given by

$$\chi = N \sigma z \quad (2.21)$$

The radiation traps heat up the atmosphere and causes the ionization of atmospheric constituents. The rate of ionization,  $R_i$ , is the product of the radiation intensity  $I$ , the gas concentration  $N$ , the photo-absorption cross-section,  $\sigma$ , and the ionization coefficient  $\eta'$

$$R_i = IN\sigma\eta' \quad (2.22)$$

The peak of  $R_i$  occurs at unity optical depth. Radiation of all wavelengths reaches F2 region (greater or equal to 200km) while the range of wavelength 20-91nm contribute to F1 (140-200km) ionization. At night these layers merge into what is commonly called F layer. Electrons are much more numerous in F2 than they are in F1 in the day. E region (90-140km) comes from the more penetrating part of the extreme ultraviolet radiation, (EUV), between roughly 80-103nm and X-rays from 1-10nm wavelength. Lower down in the atmosphere, in the D region (approximately 70-90km) the only surviving ionizing radiations are EUV at wavelength greater or equal to 103nm and X-rays of wavelength 0.2-0.8nm. (Wayne, 1993).

During the day the ionized layers exist between about 70 to 600km. The electron density  $N$  is of the order  $10^{10}$  to  $10^{12}$  electrons per cubic metre. The electron

concentration varies with the time of the day, season and over periods of several years depending on solar activity.

## 2.11 PROPERTIES OF IONISED MEDIUM

The motion of electrons in the ionosphere is very important. The equation of motion for a single electron of charge  $e$  and mass  $m$  with velocity  $v$  is

$$\frac{mdv}{dt} = -eE \quad (2.23)$$

$E$  is the electric field acting upon it. If the electric field is sinusoidal then the equation becomes

$$j\omega mv = -eE \quad (2.24)$$

For  $N$  electrons per cubic metre, the induced current in the ionized gas is

$$J = -evN$$

$$\text{Therefore } J = \frac{e^2 NE}{j\omega m} \quad (2.25)$$

$$\text{From Maxwell's curl equation } \nabla \times H = j\omega\epsilon_0 E + J \quad (2.26)$$

$$\nabla \times H = j\omega E \left[ \epsilon_0 - \frac{Ne^2}{\omega^2 m} \right] = j\omega E \epsilon_i \quad (2.27)$$

where  $\epsilon_i$  is the effective permittivity of the ionosphere. Rewriting equation (2.27)

and then dividing it by  $\epsilon_0$  yields the dielectric constant of ionized medium  $k$

$$\nabla \times H = j\omega E \left[ 1 - \frac{Ne^2}{\omega^2 m \epsilon_0} \right] = j\omega Ek \quad (2.28)$$

Given that 
$$\omega_p^2 = \frac{Ne^2}{m \epsilon_0}$$

Therefore the dielectric constant can be written as

$$k = 1 - \frac{\omega_p^2}{\omega^2} \quad (2.29)$$

A plane wave propagating through a medium of ionized gas has propagation constant  $K_c = \sqrt{k} K_o$

The phase velocity of the wave in the ionosphere is  $\frac{1}{\sqrt{\mu_i \epsilon_i}}$  and  $\frac{1}{\sqrt{\mu_o \epsilon_o}}$  in vacuum.

Hence the refractive index  $n$  is

$$n = \frac{\text{velocity in vacuum}}{\text{velocity in ionosphere}}$$

but  $\mu_i \cong \mu_o$  for ionosphere

$$\text{Therefore } n^2 = 1 - \frac{Ne^2}{\omega^2 m \epsilon_0} \quad (2.30)$$

Substituting  $e = 1.6 \times 10^{-19} \text{C}$ ,  $m = 9.1 \times 10^{-31} \text{kg}$  and  $\epsilon_0 = 8.85 \times 10^{-12} \text{Fm}^{-1}$

$$n = \sqrt{1 - \frac{81 N}{f^2}} \quad (2.31)$$

If a plane wave from space is incident normally on the ionosphere in which the electron density increases with depth, wave propagation ceases and the wave is

reflected back when the dielectric constant is equal to zero. In case of oblique incidence, as  $N$  increases with depth,  $k$  decreases and the wave refracts. The angle of refraction at different layers of the ionosphere increases. If the angle of refraction reaches  $\pi/2$ , the wave gets lost in space. According to Snell's law,  $\sin i/\sin r = k$ . If  $\sin i = k$ , then wave reflects. The plasma frequency for  $k = 0$  is known as critical frequency  $f_c$  and it occur at critical electron concentration  $N_c$ .

Given that  $f_c = 9\sqrt{N}$

$$n = \sqrt{1 - \left[\frac{f_c}{f}\right]^2} \quad (2.32)$$

## 2.12 MAGNETO-IONIC THEORY AND APPLETON-HARTREE EQUATION

When a linearly polarized wave passes through an assembly of charged particles in the presence of a magnetic field  $B$ , the magnetic field causes the particles to rotate. The particles also radiate wavelets and the fields of the wavelets rotate like the charged particles. The resultant wave has its electric field rotating so that the polarization is either the same or different from that of the original wave. If the original wave has its electric field rotating in clockwise sense, the magnetic field makes the charges to rotate in the same sense and the charge radiates wavelets with the same kind of rotation. The addition of these wavelets with the original wave produces a resultant field, which rotates in the clockwise sense. In this case, the polarization has not changed and the wave is a characteristic ordinary wave. The second characteristic wave has both the

original wave and the wavelets rotating in the anticlockwise sense. The resultant wave is known as extraordinary wave. The complex refractive index,  $n$ , at angular frequency  $\omega$  is given as (Hall and Barcley, 1991)

$$n^2 = 1 - \frac{X}{1 - iZ - \left[ \frac{Y_T^2}{2(1 - X - iZ)} \right] \pm \left[ \frac{Y_T^4}{4(1 - X - jZ)^2} + Y_L^2 \right]^{\frac{1}{2}}} \quad (2.33)$$

where the dimensionless quantities  $X$ ,  $Y$  and  $Z$  are defined as follows

$$X = \frac{Ne^2}{\epsilon_0 m \omega^2} \quad (2.34a)$$

$$Y_L = \frac{eB \cos \vartheta}{m \omega} \quad (2.34b)$$

$$Y_T = \frac{eB \sin \vartheta}{m \omega} \quad (2.34c)$$

$$Z = \frac{\nu}{\omega} \quad (2.34d)$$

where  $\vartheta$  is the angle between the propagation direction and the geomagnetic field,  $\nu$  is the electron collision frequency,  $N$  is electron concentration,  $e$  and  $m$  are the electronic charge and mass respectively and  $\epsilon_0$  is the permittivity of free space, and  $\omega$  is the angular wave frequency.

Two special cases of this equation are possible namely the quasi-longitudinal and the quasi-transverse approximations, and in each case the collision term  $Z = 0$ .

For quasi-transverse propagation,  $\theta=90^\circ$  and  $Y_z = 0$ . The Appleton-Hartree equation reduces to the following forms for the upper and lower signs respectively.

$$n_{upper}^2 = 1 - X \quad (2.35)$$

$$n_{lower}^2 = 1 - \frac{X(1 - X)}{1 - X - Y_T^2} \quad (2.36)$$

The electrical field oscillates parallel to the earth's magnetic field and therefore is unaffected by the earth's magnetic field. This is referred to as the upper sign. The cut off frequency which depends on the electron density of the ionospheric layer occurs when the refractive index  $n_{upper}^2 = 0$ , that is  $X = 1$

The electrical fields of the extraordinary wave oscillate perpendicular to the earth's magnetic field and therefore is affected by it. This is referred to as the lower sign. The refractive index  $n_{lower} = 0$  for which  $X = 1 + Y$  and  $X = 1 - Y$  and resonance for  $X = 1 - Y^2$

For quasi-longitudinal propagation,  $\theta = 0^\circ$  and  $Y_T = 0$ . The Appleton-Hartree equation reduces to

$$n^2 = 1 - \frac{X}{1 \pm Y} \quad (2.37)$$

The complex refractive index expressed in equation (2.33) can also be written as

$$n = \mu - i\chi \quad (2.38)$$

where  $\mu$  is the actual wave refractive index and  $\chi$  is responsible for wave absorption in the ionosphere. The vibration of an electric field of a wave emerging from the ionosphere is written as

$$E = E_o \exp(-k\chi L) \exp i(k\mu L) \quad (2.39)$$

where  $k\chi L$  is the decay in amplitude and  $k\mu L$  is the phase change for a distance  $L$ .

### 2.13 FARADAY ROTATION

When a linearly polarized wave enters the ionosphere it splits into two characteristic waves, the ordinary and the extraordinary waves and each has its own polarization and propagation constant. The two waves have different phase velocities so that their phase difference changes as they travel. At their exit from the ionosphere the two waves combine but because of the phase difference, the resulting polarization is not the original polarization.

A linearly polarized wave is a superposition of two oppositely circularly polarized waves. The ordinary and the extraordinary waves that the linearly polarized wave decomposed to in the ionosphere are two oppositely circulating circularly polarized waves. The ordinary wave is circularly polarized with a right-hand sense while the extraordinary wave is circularly polarized in the left-hand

sense. For a path length  $L$  in the ionosphere the angle of rotation,  $\psi$  of the wave is given by (Maral and Bousquet, 1998)

$$\psi = \arctan \left( \frac{\sin \Delta \phi}{\tan \alpha_e} \right) \quad (2.40)$$

where  $\Delta \phi$  is the difference between satellite longitude and site longitude and  $\alpha_e$  is the site latitude. The resulting XPD and mismatch loss are respectively written as

$$XPD = -20 \log \tan \psi \quad (2.41)$$

$$\text{and } L_{PT} = -20 \log \cos \psi \quad (2.42)$$

## 2.14 POLARISATION LOSS FACTOR

A receiving antenna will extract maximum energy from an oncoming radio wave when the polarization of the wave matches that of the receiving antenna. In most cases, the polarization of a wave does not always match that of the antenna. Polarization loss factor is the loss due to mismatch between the two polarizations. In a link with circular polarization, the transmitted wave is circularly polarized only on the axis of the antenna and becomes elliptically polarized off this axis. Propagation through the atmosphere can also change circular into elliptical polarization. In a linearly polarized link, the wave can be subjected to a rotation of its plane of polarization as it propagates through the ionosphere. Therefore, the polarization of the receiving antenna may not be aligned with that

of the incident wave. If the polarization of the electric field of the incident radio wave and that of the receiving antenna are expressed as (Balanis, 1982)

$$\mathbf{E}_i = a_i E_i \quad \text{and} \quad \mathbf{E}_r = a_r E_r \quad \text{respectively}$$

where  $a_i$  and  $a_r$  are unit vectors. The loss due to the mismatch is given as in equation (2.42) where  $\psi$  is the angle between the two unit vectors. In the case where a circularly polarised antenna receives a linearly polarised wave or a linearly polarised antenna receives a circularly polarised wave, the polarization angle is  $45^\circ$  and the loss factor is 3dB (Balanis, 1982, Maral and Bousquet, 1998).

## 2.15 CROSS POLARIZATION DUE TO RAIN

Raindrops cause attenuation of radio wave propagating through them. Apart from attenuation, they also bring about the transfer of electromagnetic energy from one polarization to another. Rain introduces cross-polarization as a result of differential attenuation and differential phase shift between two orthogonal characteristic polarizations. These are due to the non-spherical shape of raindrops.

The amount of differential attenuation and differential phase shift experienced by radio waves passing through an assembly of raindrops depend on a number of factors, which include the drop size distribution, frequency, and rainfall rate. Maximum effects will be observed when the electric field vector of the wave propagates parallel to the raindrop's major axis

## 2.16 DIELECTRIC PROPERTIES OF WATER

In the calculation of the scattering properties of hydrometeors, the knowledge of their dielectric properties is fundamental. Dielectric properties are usually expressed by the complex dielectric constant

$$E(r) = E'(r) - iE''(r) \quad (2.43)$$

$$\text{or the complex refractive index } N(r) = N'(r) - iN''(r). \quad (2.44)$$

Their imaginary part is related to the loss in the medium while the real part is responsible for the change of phase of the electromagnetic wave passing through it. The two quantities are simply related by  $N = \sqrt{\epsilon}$ . The dielectric property of liquid water for wavelengths longer than 1mm is due to the polar nature of the water molecules whereas for wavelengths shorter than 1mm, the dielectric properties is governed by various kinds of resonance absorptions in the molecule. The dielectric property depends not only on frequency but also on temperature. Although, various kinds of electrolytes in water affect the dielectric property by their ionic conductivity, its effect is negligible at microwave and millimeter wave bands. Ray (1972) obtained an empirical model for the complex refractive index of water in terms of its complex permittivity that is applicable over a temperature range of  $\theta = -20^\circ$  to  $250^\circ\text{C}$  and for wavelengths from  $2\mu\text{m}$  to several hundreds of metres. Ray (1972) also obtained an empirical model of the complex refractive index of ice. The procedure for the construction of the model is similar to that for water.

The exact shape of a raindrop at any instance of time is a function of a complex mixture of surface tension and aerodynamic forces as they fall to the ground. Raindrop size ranges from very small to fairly large ones. The smallest drop may be equivalent to those formed in clouds. The largest drops will not exceed 4mm in radius since the drops with radii greater than 4mm are hydrodynamically unstable and break up.

Falling raindrops often assume a nearly spherical shape. The aerodynamic force on the raindrops provide the major orientation force for the raindrops. The larger the drops, the more they can be distorted from a spherical shape. The raindrops may vibrate and oscillate while falling but the net shape is either oblate or prolate (fig.2.5) spheroid, with the oblate having higher occurrence likelihood. Nelson and Gokhale (1972) showed that the natural oscillation frequency of raindrop shape between oblate and prolate spheroid is expressed as

$$F = 11.7d^{-1.47} \text{ Hz} \quad (2.45)$$

where  $d$  is raindrop diameter in cm.

Attenuation of a linearly polarized radio wave passing through a raindrop depends on the relative orientation of the electric field and the raindrop major axis. Radio wave propagating with its electric field vector parallel to the major axis of the raindrop would experience much attenuation.

## 2.18

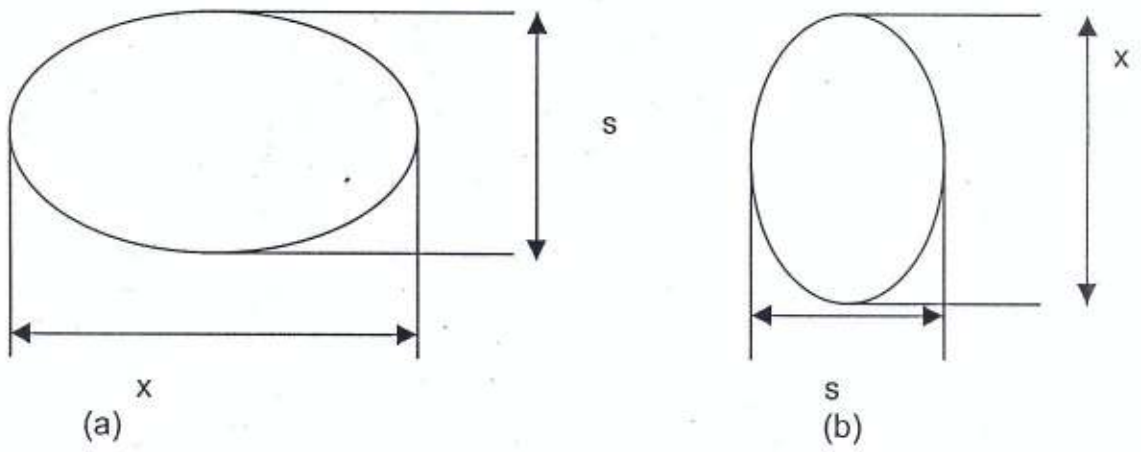
### CANTING ANGLE OF RAINDROP

The axes of non-spherical raindrops in the atmosphere are not always perfectly aligned in the vertical direction but cant away due to various aerodynamic forces acting on the raindrops. The angle of raindrops axis measured from the vertical differs with the raindrops, thereby forming a distribution whose mean is near the vertical. Saunders (1975) made the first measurement and found that the distributions are almost normal with mean canting angle of  $+7^\circ$ . About 40% of the drops have positive angles greater than  $15^\circ$  while 25% have negative angles less than  $-15^\circ$ . Ugai and Akimoto (private correspondence) proposed a canting angle model represented graphically in figure 2.6. The canting angle  $\alpha$  is made up of two angle components  $\alpha_1$  and  $\alpha_2$ , where  $\alpha_1$  is the angle between the vertical and the trace of fall and  $\alpha_2$  is the angle between the trace of fall and the drop axis.  $\alpha_2$  is called the angle of drop oscillation. These angles depend on wind direction. For a given earth-satellite path, the radio wave will suffer much attenuation and phase shift if it propagate parallel to the major axis of raindrop.

## 2.19

### RAINDROP FALL VELOCITY

The fall velocity of a raindrop increases as the drop size increases. At a radius of 2.5mm, the fall velocity is about 9m/s. Further increase in the raindrop size result in a slight increase in the fall velocity. An approximate maximum velocity occurs before a fairly large raindrop break up. Terminal velocity is an essential parameter in calculating the rainfall rate. The rainfall rate is the rate at which



$x$  =major axis and  $s$  =minor axis

Fig 2.5 Raindrop shape (a) oblate spheroidal raindrop

(b)Prolate spheroidal raindrop

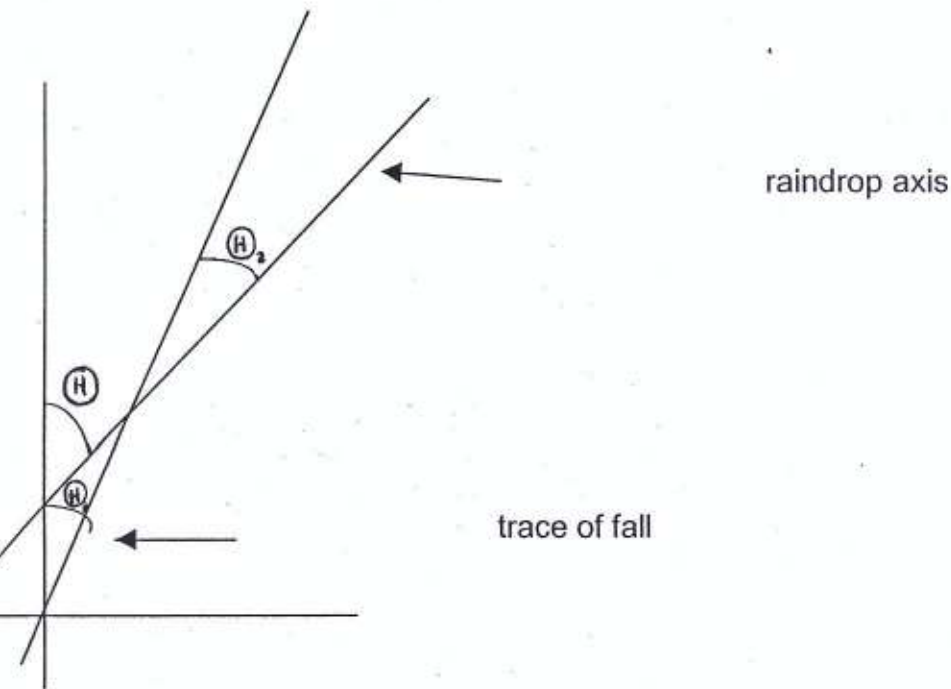


Fig.2.6 A model of raindrop canting

water reaches the ground or the rate of accumulation of water per unit time. According to Battan (1973), the contribution of individual raindrop or ice particle of mass  $m$  to the precipitate rate is

$$R = m(v - u) \quad (2.46)$$

where  $v$  is the terminal velocity of the individual raindrop or ice particle and  $u$  is the updraft rate. The rainfall rate is related to specific attenuation via a power law by

$$A = aR^b \text{ (dB / km)} \quad (2.47)$$

and to phase shift by

$$\phi = hR^k \quad (2.48)$$

where  $a$ ,  $b$ ,  $h$  and  $k$  are frequency and temperature dependent constants. The more the fall velocity the greater the rainfall rate. Consequently attenuation and phase shift become greater.

## 2.20 RAINDROPS SIZE DISTRIBUTION MODEL

Actual raindrops do not consist of spherical drops of the same size, rather a distribution of various sizes and shapes that depends on the rate of precipitation. Many investigators have used different methods to determine and calculate the drop size distributions in different climatic regions.

Laws and Parsons (1943) used a tray of fine flour exposed to rain and the size of pellets formed by raindrops was measured. The actual raindrop size was deduced by using a known relation between the dried pellet size and the raindrop size.

There are some other models such as the negative exponential distribution of Marshall and Palmer (1948), the Joss *et. al* (1968) distribution and the Lognormal distribution by Ajayi and Oslon (1985). The lognormal distribution is considered relevant because it can be used to determine tropical rainfall size distribution. The distribution is expressed by the three-parameter function given as

$$N(D) = \frac{N_T}{\sigma D \sqrt{2\pi}} \exp\left(-\frac{1}{2} \left[\frac{\ln D - \mu}{\sigma}\right]^2\right) \quad (2.49)$$

where  $\mu$  is the mean of  $\ln D$ ,  $\sigma$  is the standard deviation and  $N_T$  is the total number of drops of all sizes. These three parameters depend on climate, geographical location and rainfall type and are expressed as

$$N_T = a_o R^o \quad (2.50a)$$

$$\mu = A_\mu + B_\mu \ln R \quad (2.50b)$$

$$\sigma^2 = A_\sigma + B_\sigma \ln R \quad (2.50c)$$

Ajayi and Adimula (1989) reported that the lognormal model is more adequate for widespread, shower and thunderstorm rain in the tropics than other models.

## 2.21 SLANT PATH IN THE RAIN REGION

Temperature decreases with height in the lower atmosphere and the locus of the points where temperature reaches zero is called the zero degree isotherm. Above this no liquid water exist. The region of the atmosphere between the zero degree isotherm and the sea level is referred to as the rain region. In figure 2.7, A and C are regions of frozen and liquid precipitate respectively while B is the rain height and D is the earth-space path. The rain height is given by

$$h_R = 3 + 0.028 \alpha_e \quad (2.51)$$

if  $\theta$  is less than  $\alpha_e$  and  $\alpha_e$  less than  $36^\circ$

$$\text{or } h_R = 4 - 0.075(\alpha_e - 36) \quad (2.52)$$

if  $\alpha_e$  is greater or equal to  $36^\circ$ ,

The slant path length  $L_s$  below the rain height for  $\theta$  greater or equal to  $5^\circ$  is (ITU-R, 2000)

$$L_s (km) = \frac{h_R - h_s}{\sin \theta} \quad (2.53)$$

For  $\theta$  less than  $5^\circ$

$$L_s (km) = \frac{2(h_R - h_S)}{\left[ \sin^2 \theta + \frac{2(h_R - h_S)}{R_e} \right]^{1/2} + \sin \theta} \quad (2.54)$$

where  $\theta$  = elevation angle at the site.

$h_s$  = the station elevation above sea level

$R_e = 8500\text{km}$  (ITU-R, 2000), the effective radius of the earth. The horizontal projection,  $L_G$ , of the slant-path length is given as

$$L_G (km) = L_S \cos \theta \quad (2.55)$$

## 2.22 CROSS POLARISATION ISOLATION AND DISCRIMINATION

Cross polarization, according to Maral and Bousquet (1998) was identified as energy transferred from one polarization to an orthogonal polarization which occurs either as a result of the rotation of the plane of polarization or because of the passage of the electromagnetic wave through an assembly of hydrometeors. Figure 2.8 shows a transmitted and a received signal of different polarizations.  $E_V$  and  $E_H$  are electric fields radiated from the antenna with vertical and horizontal polarizations respectively.

Cross polarization discrimination  $XPD$  is the ratio of the electric field of the targeted polarization  $E_{TP}$  radiated from the channel aimed at, to the electric

field from the same channel which is received with orthogonal polarization  $E_{OP}$ . Mathematically, it is written as

$$XPD = 20 \log \left( \frac{E_{TP}}{E_{OP}} \right) \quad (2.56)$$

It can also be defined as written in equation (2.41) where  $\psi$  is the polarization mismatch angle. If the targeted polarization is vertical,

$$XPD = 20 \log \left( \frac{E_{VV}}{E_{VH}} \right) \quad (2.57)$$

where  $E_{VV}$  is electric field radiated and received with vertical polarization while  $E_{VH}$  is the electric field radiated with vertical polarization but received in horizontal polarization. If the targeted polarization is horizontal,

$$XPD = 20 \log \left( \frac{E_{HH}}{E_{HV}} \right) \quad (2.58)$$

where  $E_{HH}$  is electric field radiated and received with horizontal polarization while  $E_{HV}$  is the electric field radiated with horizontal polarization but received with vertical polarization.

Cross polarization isolation  $XPI$  is the ratio of the electric field transmitted and received in the targeted polarization from the channel aimed at, to the electric field transmitted in orthogonal polarization from another channel but received with the targeted polarization by the same receiving antenna.

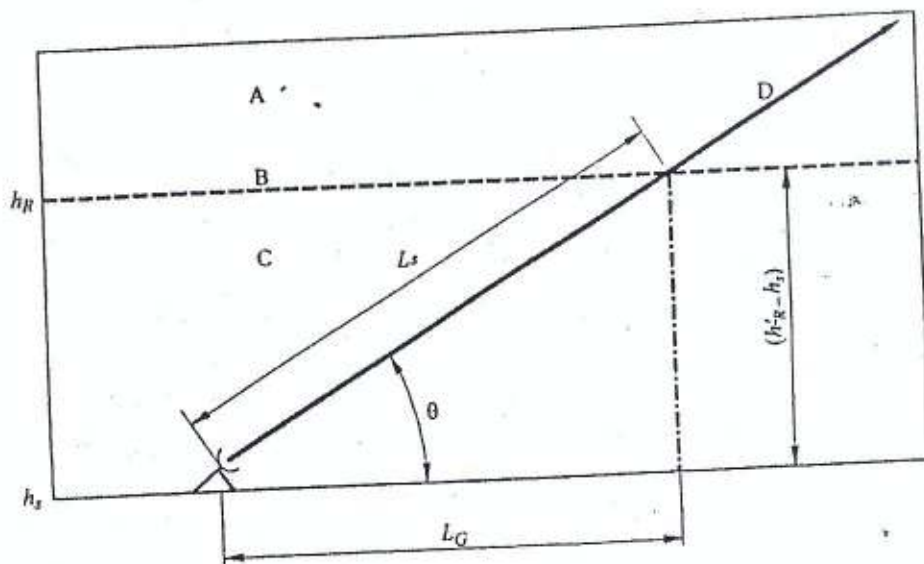


Fig.2.7 Schematic representation of earth –space path

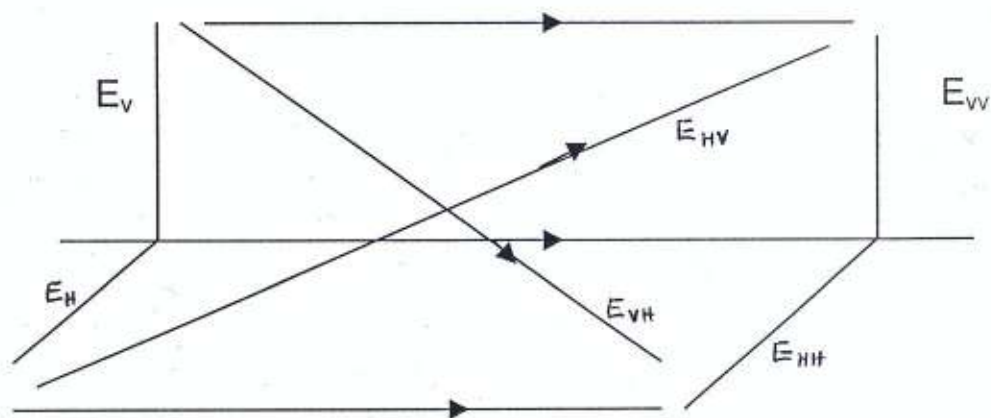


Fig2.8 Schematic representation of crosspolarisation isolation and crosspolarisation discrimination

For signal received with vertical polarization

$$XPI = 20 \log \left( \frac{E_{VV}}{E'_{HV}} \right) \quad (2.59)$$

For signal received with horizontal polarization.

$$XPI = 20 \log \left( \frac{E_{HH}}{E'_{VH}} \right) \quad (2.60)$$

$E'_{HV}$  is electric field radiated with horizontal polarization but received with vertical polarization while  $E'_{VH}$  is electric field radiated with vertical polarization but received with horizontal polarization.

## CHAPTER 3

### 3.0

### EARTH STATION

An earth station is any transmitting or receiving system that sends signal to or receives signal from a satellite. The earth station may be located on a ship at sea or on an aircraft, but it is still called an earth station since it forms the earth-based end of the earth-space link. The most visible part of an earth station is usually the antenna, which may be as large as 30m in diameter in the Intelsat network, or as small as 0.15m for reception of direct broadcast satellite television (DBS-TV). One feature common to all earth stations is the need to achieve a low system noise temperature and high gain.

The complexity of the earth station depends on the service to be provided and the expected figures of merit. The simplest station permits reception only e.g. television receive only (TVRO) and is equipped with a parabolic antenna which may have diameter less than one metre. The earth station used for this work composed of among others, a 3.0m parabolic dish and a logic digital receiver. Large antenna, which may require very high gain and low noise temperature, are capable of carrying large numbers of telephone, television, audio and data channels simultaneously. A high volume of traffic is needed to recover the cost of establishment and maintenance of a large station.

The TVRO is the receiving earth station that receives television channels only. Some TVRO receives audio channels as well as television channels. The TVRO is the domestic earth station commonly seen around. The compositions of

a TVRO, like the one used for this study, are antenna, low noise block converter (LNB), feed horn, RF cable, dish pole, receiver and monitor. Sometimes positioner is used to change the dish focus from one satellite to another.

### 3.1 MICROWAVE ANTENNA

At frequencies greater than 1GHz, antennas are usually significantly larger than the wavelength and this allows techniques akin to those of optical devices such as reflectors and lenses to be used. Microwave antenna includes the parabolic reflector, horns and omni slots. The commonest microwave antenna is the parabolic reflector. The basic property of a parabolic reflector is that it converts a spherical wave emanating from a point source placed at the focus into a plane wave. Conversely all the energy received by the dish from a distant source is focused to a single point at the focus of the dish. Mathematically, the geometry of a dish is written as

$$Y^2 = 4fx \quad (3.1)$$

where  $f = \frac{D_A^2}{16d}$  and  $d$  is the parabolic dish depth

This can be used to graphically determine the dish profile before its formation.

### 3.2 ANTENNA SIZE

This is a very important factor since it determines the maximum gain that can be achieved at a given frequency and the beam width resulting. The gain of

an antenna, according to Maral and Bousquet (1998) is the ratio of the power radiated (or received) per unit solid angle by the antenna in a given direction to the power radiated (or received) per unit solid angle by an isotropic source fed with the same amount of power. The gain is maximum in the direction of maximum radiation. The actual gain obtained is given by

$$G_{\max} = \frac{4\pi}{\lambda^2} A_e \quad (3.2)$$

for a reflector of diameter  $D_A$  the effective aperture  $A_e$  is

$$A_e = \eta A \quad (3.3)$$

where  $A$  is the actual geometric surface and  $\eta$  is the efficiency of the antenna.

Therefore, maximum gain is

$$G_{\max} = \left( \frac{\pi D_A}{\lambda} \right)^2 \eta \quad (3.4)$$

The efficiency of a parabolic dish, in the receiving mode, is the ratio of the energy received from space to the energy reflected into the feed horn placed in its focus.

In the transmit mode, it is the ratio of energy radiated from the point source at the focus to the energy reflected by the parabolic dish. The efficiency of an antenna

is a product of some factors, which are the illumination efficiency,  $\eta_i$ , spillover efficiency,  $\eta_s$ , blockage efficiency,  $\eta_b$ , and surface finish efficiency,  $\eta_f$ . Therefore

$$\eta = \eta_i \times \eta_s \times \eta_b \times \eta_f \quad (3.5)$$

### 3.2.1

## ILLUMINATION EFFICIENCY

The illumination efficiency,  $\eta_i$ , specifies the illumination of a dish with respect to uniform illumination. Uniform illumination ( $\eta_i=1$ ) occurs when every part of the dish surface is equally illuminated by the radiation from the feed but this is not possible because the focal point is farther from the dish edge than its center. Since radiation power diminishes with the square of the distances, less energy arrives at the edge than at the centre. This loss is referred to as illumination loss.

### 3.2.2

## SPILOVER EFFICIENCY

Maral and Bousquet (1998) defined the spillover efficiency as the ratio of the energy radiated by the primary source, which is intercepted by the reflector to the total energy radiated by the primary source. The difference constitutes the spillover energy. According to Pratt and Bostian (1986), spillover efficiency is  $1 - \text{spillover energy}$ . The larger the angle under which the reflector is viewed from the source, the greater the spillover efficiency. The closer the focal point the larger the angle becomes.

### 3.2.3

## SURFACE FINISH EFFICIENCY

An understanding of the degree of accuracy required in a dish is important for two reasons. It enables the maximum frequency for efficient operation of a given dish to be determined. It also enables an estimate to be made of how construction tolerances influence the gain and hence the ease with which dishes

can be constructed. The reduction in gain due to surface irregularities depends upon two factors.

The amount by which the surface deviates from a true parabola.

The ratio of such deviation to the wavelength of operation.

The surface finish efficiency takes account of the effect of surface roughness on the gain of the antenna. The actual parabolic profile differs from the theoretical one. The effect on the on-axis gain is of the form (Maral and Bousquet, 1998)

$$\eta_f = \exp\left(-B\left[\frac{4\pi E_m}{\lambda}\right]^2\right) \quad (3.6)$$

where  $E_m$  is the root mean square of the surface irregularity, which is the deviation between actual and theoretical profiles measured perpendicularly to the concave face and B is a coefficient whose value less or equal to 1. The value of B varies as a function of  $\frac{f}{D_A}$ . With  $\frac{f}{D_A} = 0.7$ , B is of the order of 0.9. The  $\frac{f}{D_A}$  of the dish constructed for this study is 0.36 and hence B is taken as 0.46.

From studies into the manufacture of parabolic reflectors by various methods, it has been found that relative error,  $\frac{E_m}{D_A}$ , is nearly a constant quantity, peculiar to a particular manufacturing technique. The ratio of the root mean square of surface error to the reflector diameter is called the relative error. For most common methods of reflector manufacture in quantity (Sazonov, 1990)

$$\frac{E_m}{D_A} = 0.4 \times 10^{-3} \quad (3.7)$$

which means that for a 3.0m dish the maximum deviation on the surface contour is about  $E_m = 1.2\text{mm}$ . The surface finish efficiency used for this study is approximately one (1)

In order to obtain  $\frac{E_m}{D_A}$  less or equal  $0.4 \times 10^{-4}$ , a better reflector technology is essential which often involve surface fitting. Very precise parabolic reflectors of a smaller size can be fabricated by spinning. The resulting relative accuracy is

$$\frac{E_m}{D_A} = 2.4 \times 10^{-5}$$

### 3.2.4 DISH OBSTRUCTION

Fitting a feed in front of the dish inevitably obscures part of the dish and therefore causes some loss in gain. Aperture blocking is accounted for by introducing a blockage factor ( Sazonov, 1990)

$$\eta_b \approx \frac{A - A_b}{A} \quad (3.8)$$

where  $A$  is the overall surface area of the dish and  $A_b$  is the area blocked by the feed and its support structure. Aperture blockage reduces gain in two ways. It leads to rise in scatter signal and consequently the noise temperature of the antenna. Secondly, the area of the aperture for maximum gain is reduced by the blockage factor. The blockage factor of the dish used for this study is 0.98 where

$A = \frac{\pi D_A^2}{4} = 7.0695m^2$ , the radius of the LMB holder is 0.08m, the length and thickness of each tripod are 1.6m and 0.02m respectively.

### 3.3 METHODS OF CONSTRUCTION.

The antenna for this present study was constructed by the method of moulding.

#### 3.3.1 MOULDING

A 3.0m dish was constructed using a concrete mould. After washing the mould surface with a mixture of water and detergent and allowing to dry, a cake of soap dipped in water was rubbed on it leaving the surface with dispersed soap leather. After about ten minutes, resin solution (phenol-formaldehyde) was applied to the surface with the aid of a medium size painting brush. Layers of aluminum foil were neatly laid on the mould followed by layers of fiberglass. The resin held the foil to the mould throughout the period of the construction while the soap leather provided easy removal of the dish from the mould after construction. More resin solution was now spread on the fiberglass. The parabolic dish metal frame was placed on the mould, followed by other layers of fiberglass before the addition of resin solution to ensure firm grip between the fiber, aluminum foil and the metal frame. After five hours, the dish was sufficiently dry and ready for use. After removal the edge was trimmed to shape. The front painted white while the back was painted gray. The mould was again washed as well as the brush.

Relevant precautional measure taken was the washing of hands each time the resin solution came in contact with them.

Dishes up to about a metre in diameter are usually made from solid materials. Aluminum is frequently used because of its lightweight and durability. Unplated materials such as iron and steel are likely to corrode and thereby result in deformation of the dish surface. Fibre material is preferred since it prevents corrosion. Obviously windage problem increases rapidly with dish size. Mesh wire presents an advantage over solid materials in this regard but the wire – to – hole ratio must be high else much signal will be lost. It is obvious that a solid material reflects better than a surface full of holes but if the size of the hole is kept to a small fraction of the wavelength that is being reflected, the hole will cause only a moderate reduction in efficiency.

Fiber material is the major material used for this casting. It is made up of alkaline free glass known as E-glass. This material has an outstanding electric insulating properties and chemical stability. It is in the form of thin strands and has the following properties that make it useful in the casting of parabolic reflector antenna

- The glass fiber has the ability to prevent energy loss. It is useful to enhance reflection of signals to the focal point.
- It reacts very well with resin thus producing a nearly perfect paraboloid.

- It has resistance against moderately high temperature.
- It does not shrink with age nor promote bacteria or fungal growth.
- It has resistance against rusting, chemical attack and weathering.

It has high strength to weight ratio thus the mechanical support will not be difficult.

### 3.4 FOCAL LENGTH TO DIAMETER RATIO $\left(\frac{f}{D_A}\right)$

This is a fundamental ratio that is directly related to the angle subtended by the rim of the dish at its focus and therefore the beamwidth of the feed. The ratio is an important factor in the design of feed for efficient illumination of the dish. Practically, the value of  $\frac{f}{D_A}$  ratio ranges between 0.2 and 1.0. The factors

governing the choice of  $\frac{f}{D_A}$  ratio are (RSGB, 1994)

The geometry and type of feed

The application of the dish.

The value of 0.25 corresponds to a common focal-plane dish in which the focus is in the same plane as the rim of the dish. The greater the ratio the deeper the dish becomes. The advantage of low  $\frac{f}{D_A}$  ratio is its compactness. Being short focal length dish, the combination of feed with the antenna result in a less bulky

system. Factors favouring the use of high  $\frac{f}{D_A}$  ratio are ease of construction

especially when using a mould or an existing dish, the ease of feeding due to reduced space loss and the loss incurred by the variation in the position of the feed's phase centres. Also, the beamwidth of the feed required to illuminate a dish efficiently increases rapidly as the  $\frac{f}{D_A}$  ratio of the dish is decreased. A high

$\frac{f}{D_A}$  ratio produces beamwidth for efficient illumination and thus increases the gain

of the dish. The higher the  $\frac{f}{D_A}$  ratio, the more the advantages except the

mechanical problem in supporting the feed. The  $\frac{f}{D_A}$  ratio of the dish constructed

for this work is 0.36. The beamwidth or the angle in degrees subtended at focus from the dish edge is given by (Pratt and Bostian, 1986)

$$\theta_{dB} = 2 \arctan \left( \frac{\left[ \frac{f}{D_A} \right]}{1 - \frac{D_A^2}{16 f^2}} \right) = 69.62^\circ \quad (3.9)$$

Another convenient relation by which the beamwidth can be determined is

$$\theta_{dB} = 2 \arctan \left( \frac{1}{4 \left[ \frac{f}{D_A} \right]} \right) = 69.56^\circ \quad (3.10)$$

where  $D_A = 3.0\text{m}$  and  $f = 1.08\text{m}$

The low noise block converter (LNB) is the single most important item in a typical TVRO installation as it is the most significant contributor of system noise. Modern LNB's have a noise figure of 0.025dB for C-band applications and 0.0939dB for Ku band applications. The noise figure of an LNB is a measure of how sensitive the LNB is or how much noise the LNB will add to the signal received. The lower the noise figure of the LNB, the better the LNB will be able to receive weaker signals. Noise temperature is more frequently used in satellite communication system; it is therefore necessary to convert noise figure to noise temperature (RSGB, 1994; Pratt and Bostian, 1986). The relationship between noise figure and noise temperature is given by

$$NF = \log \left( 1 + \frac{T}{T_o} \right) \quad (3.11)$$

where  $T_o$  is the reference temperature and its value is 290K

The LNB is the first electronic device in the TVRO RF signal processing chain. It performs two functions, one is to provide very low noise amplification while amplifying the input signal and the other is to convert the 4GHz or 12GHz signal to first intermediate frequency (IF) of range 950 to 1750MHz. The gain of an LNB is the amount by which the LNB amplifies the input signal, which is expressed in decibel, (dB). The input signal is very weak when it arrives at the receiving antenna and must be amplified many times before it can be transported down the coaxial cable. If the signal is not amplified, it would be absorbed by the

losses in the coaxial cable and will never reach the receiver. A typical LNB has a gain ranging between 55dB to 65dB.

A new innovation in the market is the low noise block feed horn (LNBF). This is a device that uses a simpler method for selecting the polarity by either sending 14volts up the IF cable for vertical polarization or 18volts for horizontal polarization. (Telsat communication,1996) The advantage of the LNBF over the discrete LNB/feed horn is the improved efficiency by eliminating the polariser insertion loss. A further advancement came with the advent of digital TV transmission. These are LNB that are specially developed to meet the requirement of a very low phase noise.

### **3.6 DISH FEED SYSTEM**

An ideal dish feed system should pick up signals equally well from the whole surface of the dish. The ideal dish does not exist. Feed systems that do not pick up or radiate equally well to all areas of the dish surface are said to have illumination loss. Feed systems that pick up or radiate signal outside the dish are said to have spillover loss. All practical feed systems have these problems to some degree (Fig. 3.1). A feed system with a very wide angle of radiation will have illumination loss caused by too much power concentrated at dish's centre and will also pick up back-ground noise from outside the dish surface. A practical feed takes various forms such as pyramidal, circular and sectoral feed.

This type of feed is quite common on the lower microwave bands; its main advantage is that it can be made from readily available materials. As shown in figures 3.2, the feed consists of a short length of short-circuited, circular waveguide, often made from metal pipes. A simple form of coaxial cable to waveguide transition generally used consists of a probe just less than a quarter of a wavelength long, spaced approximately a quarter of a guide wavelength from the closed end. The diameter of the guide must be chosen such that signal wavelength in the guide is less than the cut-off wavelength  $\lambda_c=1.706D_F$ . The E-plane (horizontal) and H-plane (vertical) 3dB beamwidth, in degrees is given by the values of  $29.4L/D_F$  and  $50L/D_F$  respectively (RSGB, 1994). That this differs significantly is the main disadvantage of this feed, because it results in an uneven illumination. The circular feed used for this study has internal length and diameter of 16.20cm and 6.20cm respectively. Using  $29.4L/D_F$ , the 3dB beamwidth is  $76.82^\circ$ . If the 3dB beamwidth of the dish and the feed are considered to be equivalent to the energy of the wave, then the spillover efficiency is the dish beamwidth divided by the feed beamwidth. The value of the spillover efficiency is 0.91.

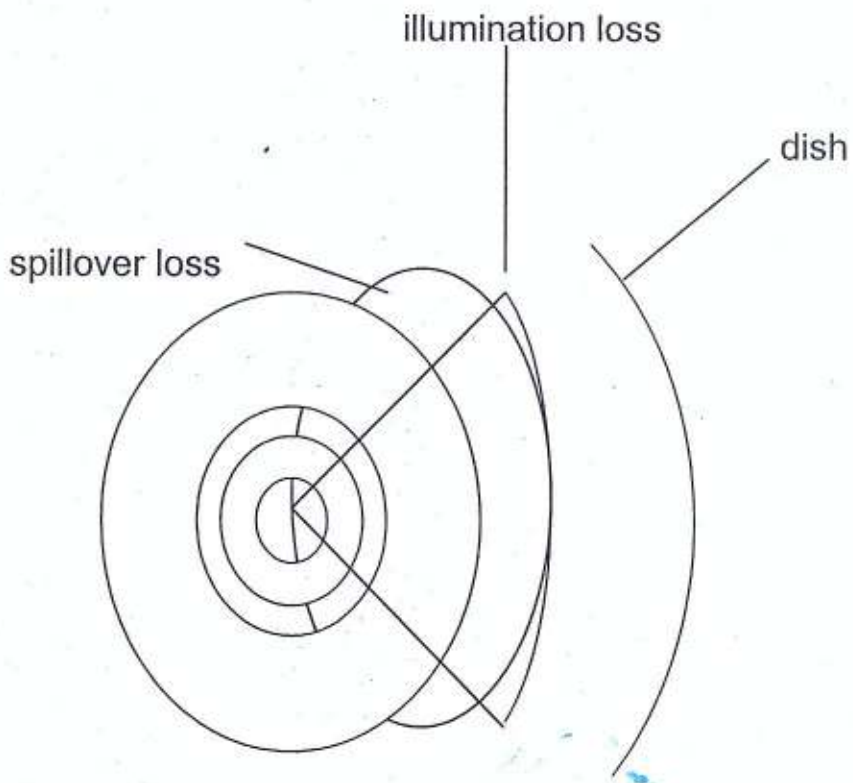


Fig 3.1 Feed pattern showing illumination and spillover losses

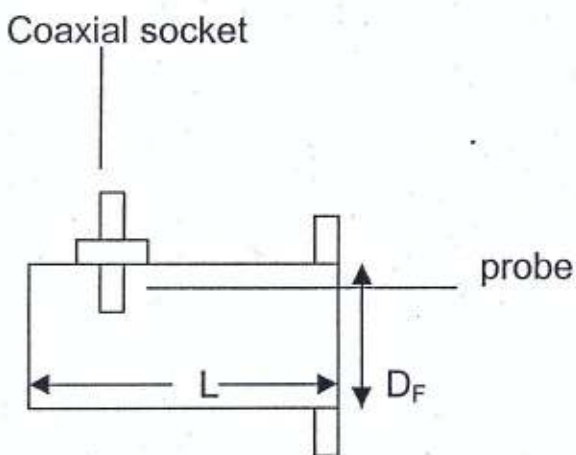


Fig. 3.2 A simple circular waveguide transition.

This is the point from which the energy radiated appears to emerge from. In practical feeds, the phase centre is rarely a point since the size of the feed is always significant in wavelength terms. The situation is further complicated by the fact that the phase centre in the horizontal (E) plane may be different from the vertical (H) plane. Multiband feeds such as log – periodic arrays suffer additional disadvantage that the phase centres will move significantly as the frequency of operation is changed. The reduction in antenna gain due to variations in the position of phase centres may likely be significant.

A polariser is an additional unit to LNB and it is used to avoid mismatch at the receiving probe. There are three main types

This has two receiving probes positioned  $90^\circ$  apart, one for vertical polarization and the other for horizontal polarization. A simple solid state switching arrangement selects either the vertical or horizontal polarization. This type has very low insertion losses with good cross-polarization isolation. The main disadvantage is that they are only suitable for either single satellite reception or reception of multi-satellites in the same orbital slot such as Astra cluster.

### **3.9.2 FERROMAGNETIC POLARISER**

This is a device, which is used to rotate the incoming signal by means of a magnetic polariser, which twists the E-field plane to that of the LNBF probe. By applying a small DC current of about 50mA or less to a specially wound coil the signal orientation that passes through the device can be rotated in a controllable manner by changing the DC polarity and the current flowing through the coil. Once set, this current must be kept constant as polarization sense is critically determined by the accuracy of the current flowing through the polariser winding. There is no moving part and the device is inserted between the LNB and the feed horn at  $45^\circ$  to the incoming signal and the rotation is set between  $-45^\circ$  and  $+45^\circ$ . This ensures that the required current is kept to a minimum and unwanted noise is also minimized. This device has insertion loss of about 0.3dB. However, since the amount of wave twisting is also dependent to some extent on frequency, they can produce poor results unless some method of trimming for different channel frequencies is allowed for on the receiver. A remote skew adjustment, which can be stored for each channel, is normally all that is required to compensate for this.

### **3.9.3 MECHANICAL MOTOR DRIVEN TYPES**

This is a motor, which physically rotates a probe according to the polarization sense selected. It works under remote servo control from the receiver. Large earth stations are often equipped with motor driven polarisers so that the antenna polarization can be changed from linear to circular. This allows the antenna to be used with more than one design of satellite. It also allows the

reception of elliptical polarization when the satellite does not radiate true circular polarization and can thus improve the isolation between two orthogonal polarization channels of a frequency reuse transmission.

### 3.1 0                      FIGURE OF MERIT

The figure of merit of a receiver and its associated antenna is the effective receiver sensitivity (*ers*) and is defined as the minimum power the antenna must receive in order that the receiver can generate an intelligible output (RSGB, 1994). To quantify this, the characteristics of the receiver, the receiving antenna and the feeder are of paramount importance

$$ers = kTB + snr - G_r + L_f \quad (3.12)$$

where  $kTB$  is the noise power generated internally by the receiver. Noise consists of all unwanted contributions whose power adds to the wanted carrier power. It reduces the ability of the receiver to reproduce correctly the information content of the received wanted carrier. The noise originates from components in the receiving equipment. The Boltzmann's constant,  $k = 1.38 \times 10^{-23}$  J/K and in decibel (dB) units, it is expressed as  $-228.6$ dB,  $B$  = receiver noise bandwidth (Hz) or the receiver i.f bandwidth,  $T$  = receiver noise temperature,  $SNR$  = signal to noise ratio of receiver,  $G_r$  = receiving antenna gain and  $L_f$  = feeder loss.

The effective receiver sensitivity, *ers*, can also be written as (UNESCO, 1996)

$$ers = \frac{G_r}{T_{sys}} (dB) \quad (3.13)$$

where  $T_{sys}$  is the system noise temperature and it is sum of the noise temperature of LNB and dish.

### 3.11 CARRIER TO NOISE RATIO

The knowledge of the carrier-to-noise ratio is used to specify the relative magnitude of the received carrier with respect to the noise present at the receiver input. Several ratios can be used.

- i. The ratio of carrier power to noise power. This is done by simply comparing the size of the same kind. It is denoted as  $\frac{C}{N}$ .
- ii. The ratio of carrier power to the spectral density of the noise  $\frac{C}{N_o}$ .

It is written as

$$\frac{C}{N_o} = \frac{C}{N} + 10 \log B(\text{dBHz}) \quad (3.14)$$

where  $B$  is the system noise bandwidth or the pre-detector i.f. bandwidth and  $N_o = kT$ . Carrier to noise spectral density can also be written in terms of down

link eirp of the transmitting and  $\frac{G}{T}$  of the receiving systems (UNESCO, 1996).

$$\frac{C}{N_o} = \text{eirp} + \frac{G}{T} - L_f - L_A - k \quad (3.15)$$

where  $L_f$  is feeder losses,  $L_A$  is free space losses and  $k$  is Boltzmann's constant

iii. The ratio of carrier power to noise temperature  $\frac{C}{T}$ . This is obtained by

multiplying  $\frac{C}{N_o}$  with Boltzmann's constant and it is expressed in W/K.

### 3.12 ANTENNA NOISE TEMPERATURE

At microwave frequency, all elements with physical temperature greater than 0°K generate noise at the system frequency within the system bandwidth. The noise temperature therefore is a function of the direction in which it is pointing, its radiation pattern and the state of the surrounding environment. It can be written as (ITU-R, 2000)

$$T_A = T_m \left( 1 - 10^{-\left(\frac{L}{10}\right)} \right) \quad (3.16)$$

L is path attenuation,  $T_m$  is the average medium temperature (K) and it can be determined empirically by

$$T_m = 1.12T_g - 50 .$$

$T_g$  is ground temperature (K) .

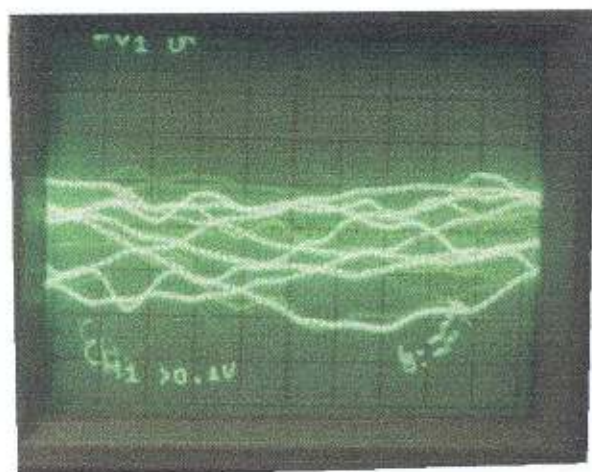
## CHAPTER 4

### 4.0 MEASUREMENTS AND CALCULATIONS

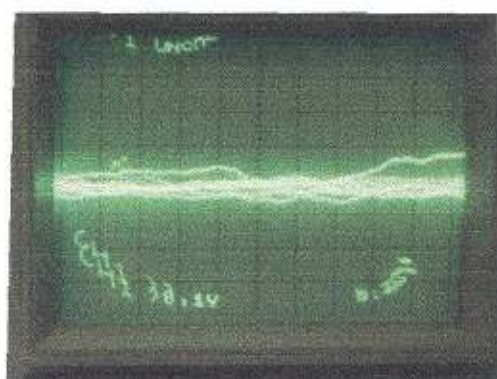
Satellite television is an amazing methodology of bringing international television entertainment to home viewers directly from orbiting satellites located high above the equator in the Pacific ocean region (POR), Indian ocean region (IOR) and Atlantic ocean region (AOR). Some of these international television channels were received at Akure (latitude  $7^{\circ} 17'N$ , longitude  $5^{\circ}12'E$ ) with the aid of a 3.0m parabolic reflector and a digital receiver. A 40MHz oscilloscope measured the amplitude of the channels' audio signal. Unlike video signal, the audio signals are sinusoidal unstable signals and therefore their waveforms were first photographed. The amplitudes of the waveforms were then measured from the pictures. Figures 4.1 (a-p) consist of the audio waveforms

Some of the channels accessed on the Intelsat satellites are

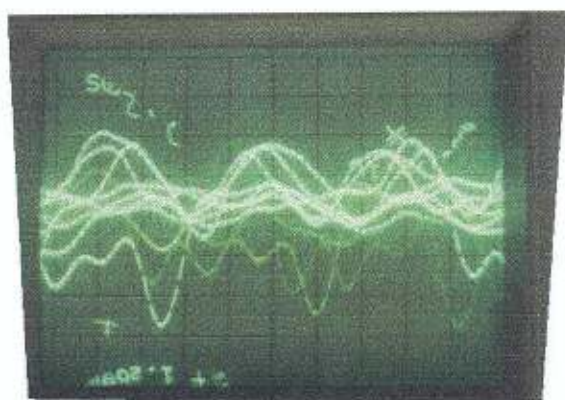
1. Independent Television, Madagascar (ITV) on Intelsat 804
2. TV Afrique channel 5 (TV5) on Intelsat 803
3. Cable Network News (CNN) on Common Feed on Intelsat 803
4. Portuguese Television (AF AFL) on Intelsat 605
5. Metro (MET) on Intelsat 605
6. East Africa Television (EATV) on Intelsat 804
7. Dutch Television (DWTV) on Intelsat 704 and
8. CFITV on Intelsat 803



(a)

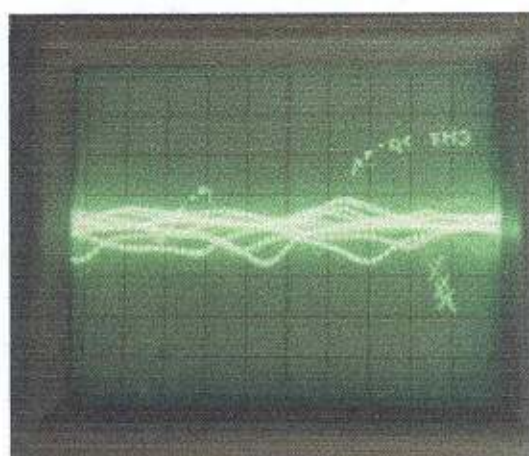


(b)

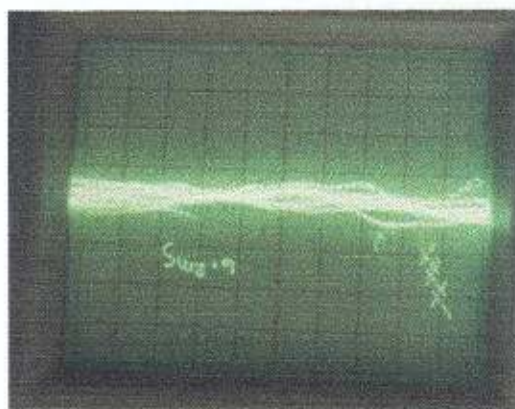


(c)

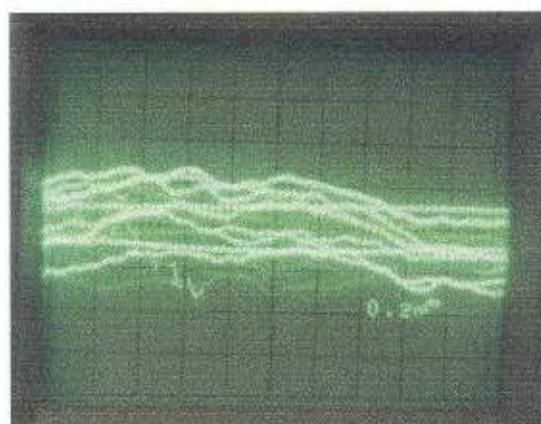
Fig.4.1 a,b,c (ITV)



(d)

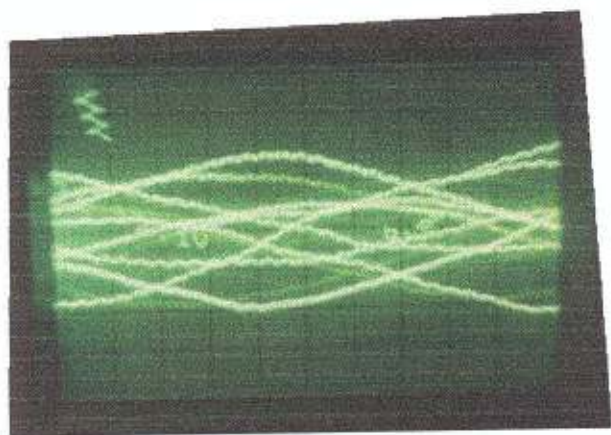


(e)

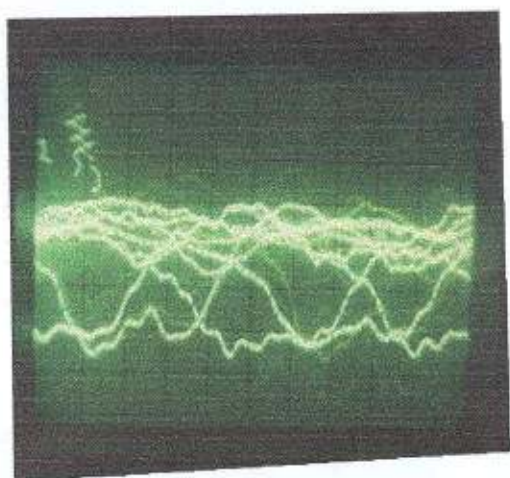


(f)

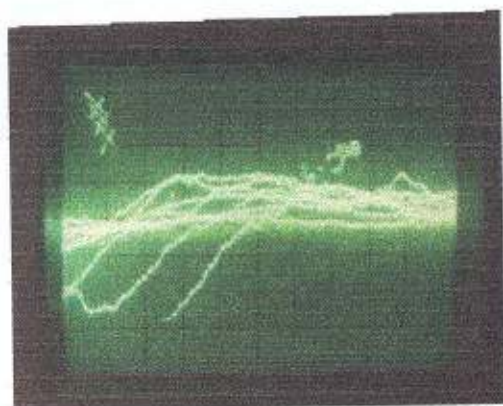
Fig 4.1 d,e,f (EATV) EAST



(g)

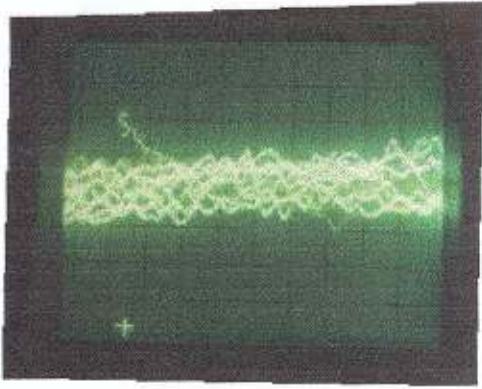


(h)

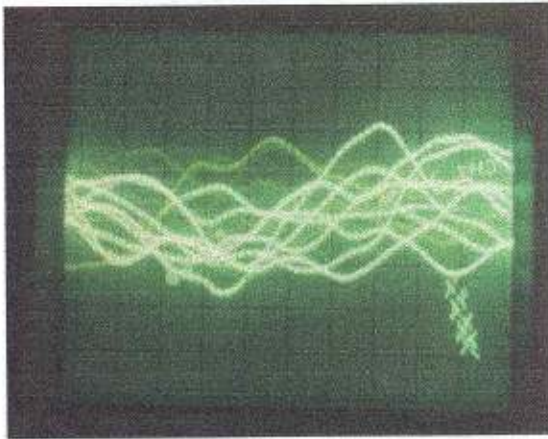


(i)

Fig 4.1 g,h,i (DWTV) GERMANY

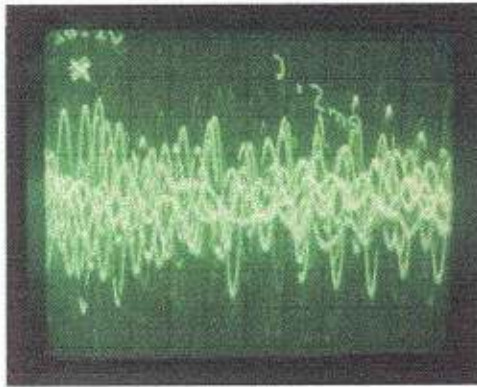


(j)

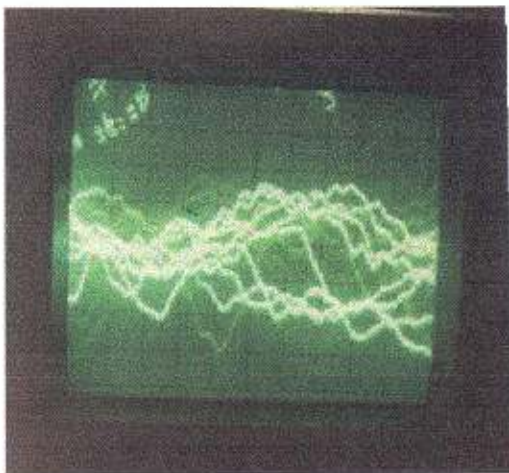


(k)

Fig.4.1 j,k, (CNN)



(l)



(m)



Fig.4.1,l,m(CFITV)

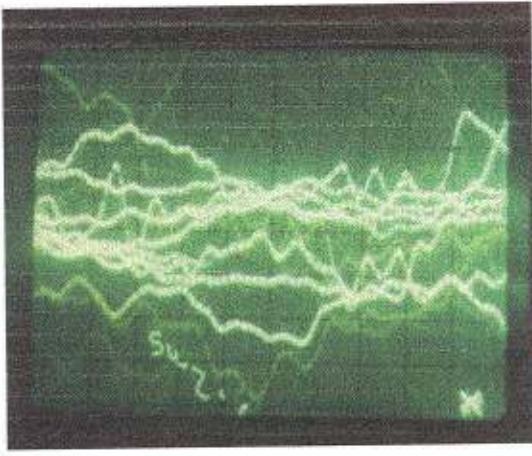


Fig.4.1 n(TV5)

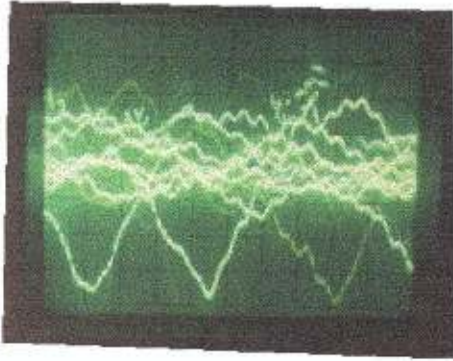


Fig 4.1 ,o (AFAFL)

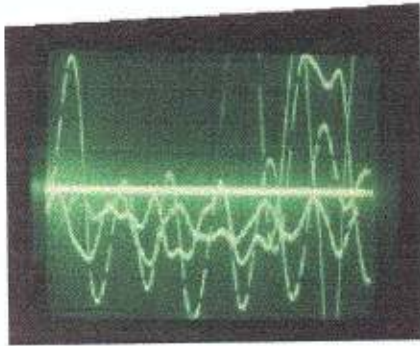


Fig. 4.1, p (MET) INDIAN

The audio waveform of each television channel was photographed repeatedly (randomly) and the average of the waveform amplitude is taken to be the signal level in voltage for the channel. The average values of the audio waveforms and the video frequencies for the satellite TV channels are shown in table 4.1. The decibel equivalent of the signal level is deduced using

$$\text{signal level (dB)} = 20 \log \left( \frac{V}{V_o} \right) \quad (4.1)$$

where  $V$  is the average recorded and  $V_o = 1\text{mV}$ , is the reference voltage

The waves of all the channels received are plane polarized though some are vertical polarized while the others are horizontal polarized. Table 4.2 consists of their equivalent decibel values, polarization and satellite positions in space.

#### 4.1 THE SIGNAL PATH LENGTH

The total path length  $r$  between the transmitting antenna and the receiving antenna is given as

$$r^2 = D_L^2 + R^2 - 2D_L R \cos \Delta\phi \cos \alpha_e \quad (4.2)$$

where  $D_L = 42.17 \times 10^6\text{m}$ , (section 2.4) distance between the satellite and the earth centre,  $R = 6.378 \times 10^6\text{m}$ , the earth radius.  $\alpha_e = 7.28^\circ\text{N}$  is the site latitude in Akure,  $\Delta\phi$  = difference between the longitudes of satellite and site. Site longitude is  $5.2^\circ\text{E}$ . When the two longitudes are in the east, the difference is  $\phi_s - \phi_e$  while it is  $\phi_s + \phi_e$  when satellite is in the west and site in the east. The values of  $r$  for the various channels appeared in table 4.3.

$$\theta = \arccos\left(\frac{D_L \sin \beta}{r}\right) \quad (4.3)$$

The values of  $\theta$  for each channel appear in table 4.3. The azimuth angle for satellites in the east is

$$A_z = 180 - \arctan\left(\frac{\tan \Delta\phi}{\sin \alpha_e}\right) \quad (4.4)$$

and  $A_z = 180 + \arctan\left(\frac{\tan \Delta\phi}{\sin \alpha_e}\right) \quad (4.5)$

is for satellite in the west. The azimuth angles for all the channels are presented in table 4.3. The free space path loss is given as

$$L_A = 20 \log\left(\frac{4\pi r}{\lambda}\right) \quad (4.6)$$

where  $r$  and  $\lambda$  are in metre. The values of the free space path loss are presented in table 4.3. The slant path length is given as

$$L_S(km) = \frac{h_R - h_S}{\sin \theta} \quad (4.7)$$

where the rain height  $h_R = 3 + 0.028\alpha_e = 3.20 km$

Table 4:1 audio signal in voltage and video signal in gigahertz

CHANNEL	ITV			EATV			DWTV			CNN	
Fig. rep	a	B	c	d	e	f	g	h	i	j	k
Signal (v)	0.360	0.160	0.500	0.180	0.120	0.260	0.440	0.360	0.400	0.240	0.400
Average signal level (v)	0.340			0.187			0.400			0.320	
Video frequency (GHz)	3.644			3.644			3.915			3.931	

CHANNEL	CFITV		TV5	AFAFL	MET
Fig. Rep	l	M	n	o	p
Signal (v)	0.580	0.440	0.540	0.580	0.800
Average signal level (v)	0.510		0.540	0.580	0.800
Video frequency (GHz)	3.650		3.650	3.644	4.131

for  $\theta$  less than  $\alpha_e$  and  $\alpha_e$  less than  $36^\circ$ .

The height of the earth station above the mean sea level  $h_s$  equals the height of the building upon which the antenna was located plus the height of the pole of the antenna i.e.  $7.2\text{m}+2.0\text{m}=9.2\text{m}$ . The values of  $L_s$  are shown in table 4.3.

## 4.2 IONOSPHERIC PATH LENGTH

The path length of the waves through the ionosphere is given as

$$L_i = \frac{h_{\max} - h_{\min}}{\sin \theta} \quad (4.8)$$

where  $h_{\max}$  (600km) is the maximum height of F2 layer and  $h_{\min}$  (70km) is the minimum height of D layer. The values of  $L_i$  for the various channels accessed are shown in table 4.4.

## 4.3 ABSORPTION INDEX

Appleton – Hartree equation (2.33) will be used to determine the attenuation due to radio wave absorption in the ionosphere. The quazi-transverse approximation (equation 2.35 and 2.36) will be applied.

For the ordinary wave

$$n_{\text{upper}}^2 = 1 - X \quad (4.9)$$

$$\text{where } X = \frac{Ne^2}{\epsilon_0 m \omega^2}$$

$$N = 10^{12} \text{ m}^{-3}, e = 1.602 \times 10^{-19} \text{ C}, m = 9.06 \times 10^{-31} \text{ kg}, \epsilon_0 = 8.85 \times 10^{-12} \text{ Fm}^{-1}$$

Table 4.2 Equivalent dB values and polarizations

CHANNEL	AFAFL	MET	ITV	EATV	CNN	CFITV	TV5	DWTV
Average signal level (v)	0.580	0.800	0.340	0.187	0.320	0.510	0.540	0.400
Equivalent dB value	35.269	38.062	30.630	25.437	30.103	34.151	34.645	32.041
Polarization	V	H	H	V	H	V	V	V
Satellite position	60.0°E	60.0°E	64.0°E	64.0°E	338.5°W	338.5°W	338.5°W	359.0°W
Satellite name	Intelsat 605	Intelsat 605	Intelsat 804	Intelsat 804	Intelsat 803	Intelsat 803	Intelsat 803	Intelsat 704

Table 4.3 Elevation angle and free space loss for frequency 22KHz

CHANNEL	AFAFL	MET	ITV	EATV	CNN	CFITV	TV5	DWTV
$r(km) \times 10^4$	3.888	3.888	3.928	3.928	3.615	3.615	3.615	3.587
Elevation angle $\theta$ (degrees)	27.142	27.142	22.927	22.927	69.096	69.096	69.096	80.111
$A_z$ (degrees)	95.108	95.108	94.388	94.388	113.430	113.430	113.430	210.100
$L_s$ (km)	6.994	6.994	8.191	8.191	3.416	3.416	3.416	3.239
$L_A$ (dB)	91.086	91.086	91.175	91.175	90.454	90.454	90.454	90.386

And  $\omega = 2\pi f = 138248$  radians .

$$n_{upper} = \pm i409.229$$

$$\text{complex refractive index } n = \mu - i\chi \quad (4.10)$$

$i\chi = \pm i409.229$ , the absorption index. The decay in amplitude is  $k_1 \chi L_i$  (dB).

$$\text{where (Andreas Schiffer, 1996)} \quad k_1 = k_o \left( 1 - \frac{\omega_p^2}{\omega[\omega - \omega_c]} \right)^{\frac{1}{2}} \quad (4.11)$$

$$\omega_p = \left( \frac{Ne^2}{m\epsilon_o} \right)^{\frac{1}{2}} = 5.6575 \times 10^7 \text{ radians (plasma frequency)}$$

$\omega_c = 8.830 \times 10^6$  radians (gyro or cyclotron frequency).  $k_o$  is the

propagation constant in vacuum.  $k_o = \sqrt{\mu_o \epsilon_o} = 3.335 \times 10^{-9}$ . Therefore

$$k_1 = 1.722 \times 10^{-7}$$

For the extraordinary wave, using equation 2.36,  $n_{lower} = \pm i404.350$

$$\text{Complex refractive index } n = \mu - i\chi$$

Therefore  $i\chi = \pm i404.350$  absorption index

The decay in amplitude of the extraordinary wave is  $k_2 \chi L_i$  (dB)

$$k_2 = k_o \left( 1 - \frac{\omega_p^2}{\omega[\omega + \omega_c]} \right)^{\frac{1}{2}} \quad (4.12)$$

where  $k_2 = 1.694 \times 10^{-7}i$ .

The attenuation due to ionospheric absorption of the ordinary and extraordinary waves are presented in table 4.4

The quasi-longitudinal approximation,  $\theta = 0^\circ$ , confirmed that the actual refractive index of the wave is approximately unity.

#### 4.4 POLARISATION MISMATCH LOSS

A plane wave is one of the waves referred to as special type of elliptical wave. This is because its plane of polarization rotates as it propagates. The rotation of its plane of polarization in the ionosphere is referred to as the Faraday rotation. The degree of rotation per unit distance in the ionosphere is more pronounced than the rotation of the plane of polarization in free space. The total degree of rotation of the plane of polarization of linearly polarized wave when propagation is from space station to earth station is given as

$$\psi_T = \arctan \left( \frac{\sin \Delta \phi}{\tan \alpha_e} \right) \quad (4.13)$$

Total loss due to polarization mismatch is

$$L_{PT} = -20 \log \cos \psi_T \quad (4.14)$$

The values of  $\psi_T$  and  $L_{PT}$  for the satellite –TV channels are shown in table 4.5

#### 4.5 CROSS POLARISATION DETERMINATION

The rotation of the plane of polarization has the tendency of leading to the transfer of energy from one polarization to an orthogonal polarization. The following steps are meant to determine the signal level at dish surface so that cross polarization at the receiving probe can be deduced. Neglecting signal loss

in the coaxial cable used to transport signal to the indoor receiver as well as the frequency improvement from the receiver. The decibel equivalent values are now taken to be the LNB output. The LNB output, ( $LNB_O$ ) is the sum of LNB gain ( $LNB_G$ ) and the signal level input into the LNB ( $LNB_i$ )

$$\text{i.e. } LNB_O = LNB_G + LNB_i \quad (4.15)$$

$$\text{thus } LNB_i = LNB_O - LNB_G.$$

where  $LNB_G = 55\text{dB}$

The  $LNB_i$  is the sum of receiving antenna gain  $G_R$  and the signal level ( $A_s$ ) received on the dish surface from space

$$\text{i.e. } (LNB_i) = G_R + A_s \quad (4.16)$$

$$G_R = 10 \log \left( \frac{\pi D_A}{\lambda} \right)^2 \eta = -66.22 \text{ dB} \quad (4.17)$$

when  $D_A=3.0\text{m}$ ,  $f=22\text{kHz}$  and  $\eta=0.5$  (ITU-R, 2000) are substituted into equation 4.17. The cross polarization discrimination is deduced using

$$XPD = -20 \log \tan \psi_T \quad (4.18)$$

The actual wave polarization targeted for each channel is calculated from equations 2.57 and 2.58. The results for  $LNB_i$ ,  $A_s$ ,  $E_{VV}$  or  $E_{HH}$  are presented in table 4.6 for all the station investigated.

Table 4.4 Ionospheric absorption for ordinary and extraordinary waves of frequency 22KHz

CHANNEL	AFAFL	MÉT	ITV	EATV	CNN	CFITV	TV5	DWTV
Path length in ionosphere $L_i$ (km)	1161.857	1161.857	1360.516	1360.516	567.430	567.430	567.430	537.993
Attenuation due to absorption for ordinary wave (dB) $\times 10^{-2}$	8.188	8.188	9.587	9.587	3.998	3.998	3.998	3.791
Attenuation due to absorption for extraordinary wave (dB) $\times 10^{-2}$	7.959	7.959	9.319	9.319	3.887	3.887	3.887	3.686
Total absorption (dB) $\times 10^{-2}$	16.147	16.147	18.906	18.906	7.885	7.885	7.885	7.477

Table 4.5 Total mismatch loss

CHANNEL	AFAFL	MÉT	ITV	EATV	CNN	CFITV	TV5	DWTV
$\Psi_T$ (degrees)	81.115	81.115	81.506	81.506	65.527	65.527	65.527	29.826
$L_{PT}$ (dB)	16.220	16.220	16.620	16.620	7.650	7.650	7.650	1.240

## 4.6

### OVERALL LOSS

There are three stages of signal loss in the propagation medium. These are losses in the ionosphere, in free space and the loss due to mismatch at the antenna. The total losses for all channels from the same satellite position are the same, since they are received at the same location and over the same path length. The losses are presented in table 4.7

## 4.7

### FIGURE OF MERIT

The approximate figure of merit of each channel can be calculated from

$$eirp = A_p + L \quad (4.19)$$

$A_p$  being the signal level (dB) of the targeted polarization ( $E_{VV}$  or  $E_{HH}$ ) on the dish surface and  $L$  is the sum of all the various losses calculated as

$$L = L_A + A_P + L_{PT} \quad (4.20)$$

The antenna brightness temperature is determined from the relation

$$T_A = T_m (1 - 10^{-L/10}) \approx 280K \quad (4.21)$$

$$T_m = 280K \text{ for cloud or } 260K \text{ for rain (ITU-R, 2000)}$$

The system noise temperature is the sum of the noise temperature of antenna and that of the LNB. The noise temperature of the LNB = 17K, therefore,

$$T_{sys} = T_A + T_{LNB} = 280 + 17 = 297K \quad (4.22)$$

The figure of merit of the TVRO then is

$$ers = \frac{G_R}{T} = \frac{-66.22}{297} = 0.222 \text{ dB/K}$$

$$\text{and } ers = 10^{-0.222/10} = 0.95 \text{ watt.}$$

The static threshold of a receiver is the minimum carrier to noise ratio it must receive to give an intelligible output. The carrier to noise ratio of each of the channel can be calculated by

$$\frac{C}{N_o} = eirp + ers - L - k \quad (4.23)$$

where  $k = 1.38 \times 10^{-23} \text{ J/k} = -228.6 \text{ dB}$  ( Boltzmann's constant.

$$\text{where } eirp = L + E_{VV} \text{ or } E_{HH} \quad (\text{dB})$$

The path loss capability,  $plc$ , is then given as

$$plc = eirp - ers \quad (4.24)$$

In this study, the actual path loss is less than the the path loss capability. Typical results for equations 4.19, 4.20, 4.23 and 4.24 are shown in table 4.7.

Table 4.6 Cross polarization discrimination

CHANNEL	AFAFL	MET	ITV	EATV	CNN	CFITV	TV5	DWTV
LNB output LNB <sub>0</sub> (dB)	35.269	38.062	30.630	25.437	30.103	34.151	34.648	32.041
Signal at LNB <sub>1</sub> input (dB)	-19.731	-16.938	-24.370	-29.563	-24.897	-20.849	-20.352	-22.959
Signal at dish surface A <sub>s</sub> (dB)	46.489	49.282	41.850	36.657	41.323	45.371	45.868	43.261
XPD	-16.119	-16.119	-16.516	-16.516	-6.837	-6.837	-6.837	4.832
E <sub>VV</sub> or E <sub>HH</sub> (dB)	2.536	2.536	2.482	2.482	3.482	3.482	3.482	2.163

Table 4.7 C/No and path loss capability

CHANNEL	AFAFL	MET	ITV	EATV	CNN	CFITV	TV5	DWTV
L <sub>A</sub> (dB)	91.086	91.086	91.175	91.175	90.454	90.454	90.454	90.386
Total ionosphere absorption (dB) x10 <sup>-2</sup>	16.147	16.147	18.906	18.906	7.885	7.885	7.885	7.477
L <sub>PT</sub> (Db)	16.220	16.220	16.620	16.620	7.650	7.650	7.650	1.240
Total Loss L (dB)	107.466	107.466	107.984	107.984	98.183	98.183	98.183	91.701
eirp (dB)	110.002	110.002	110.466	110.466	101.667	101.667	101.667	93.864
C/No	230.914	230.914	231.304	231.304	232.304	232.304	232.304	230.985
Plc	109.780	109.780	110.244	110.244	101.443	101.443	101.443	93.642

## CHAPTER 5

### 5.0 DISCUSSION AND RECOMMENDATION.

#### 5.1 DISCUSSION OF RESULTS

In the previous chapter, the following parameters of the audio signals from different eight space stations were, among others, determined.

- The free space path loss
- The signal level (dB) of the radio wave absorbed in the ionosphere.
- The polarizations mismatch loss.
- The efficiency of the parabolic dish antenna.
- The carrier to noise ratio at the receiver input.

The atmospheric induced losses; free space path loss, ionospheric absorption and polarization mismatch are greater for satellites on the eastern longitude because the channels have lower elevation angles and longer path lengths in free space and in the ionosphere. The lower the elevation angle, the longer is the path length and consequently the higher is the path loss. Also the absorption of radio wave in the ionosphere is greater in ordinary waves. This is due to the fact that the values of propagation constant and absorption index are lower in extraordinary waves compared to the values in ordinary waves (Table 4.4). The degree of Faraday rotation is greater for satellites on the eastern longitude because the path lengths are longer. Therefore polarization mismatch loss on each channel in the east is more than polarization mismatch loss on channels in the west. In each of the channels, about 75% of the losses were due to free space propagation conditions.

The signal received from space were very weak, the gain of the antenna substantially increased the input into the LNB. The International Telecommunication Union Radio (ITU-R) conservative estimate of antenna efficiency was used, however, the calculated value of the antenna efficiency is large such that it may not be lower than the conservative estimate if other factors such as focal length error and illumination loss are accounted for. The commonest defect associated with locally made parabolic dish antenna is the surface imperfection (Sazonov, 1990). This defect and its effect on the quality of the signals received were reasonably reduced to the barest minimum because resin reacts very well with fiberglass to form a nearly perfect parabola. This also implies that the method of construction is suitable. Fibre glass has resistance against moderately high temperature, and consequently the computed antenna temperature is reasonably low, thus resulting in a low system noise temperature, high carrier to noise ratio and figure of merit of the TVRO. With all this losses, the actual path loss is a little below the path loss capability, however sufficient intelligent output was produced in all the channels.

Even though the actual path loss is lower than the path loss capability in all the channels, the antenna-LNB combination improved the signal levels, compensating to a certain extent the loss in the propagation path and consequently producing intelligible output in all the channels. The effect of signal loss in the propagation path may be negligible if the signal level in the receiving system is amplified appreciably.

## 5.2

### RECOMMENDATION

Instrumentation is an important aspect of any technological research work. Spectrum analyzer is believed to be an inevitable instrument in any signal analyzes research of this sort and therefore was sort for over a period of two years. Attempt was made to construct a 1.3GHz prescaler, when we could not procure an analyzer of the required range, but the scaler ICs are not available. Finally it was agreed upon to work on only audio signals with a 40MHz oscilloscope. If a spectrum analyzer was used, the scope of the research would be broader and more information on the signal would have been made available. It is therefore being suggested that further research should include satellite video signals using spectrum analyzer. If so much signal loss as recorded in this study, takes place in clear weather, It is recommend that signal loss through clouds be investigated. It is also recommend that further work be carried out on audio signals with progressively smaller sized parabolic dishes to ascertain if the path loss capability will be less than the actual path loss.

## REFERENCES

- Ajayi, G. O. and Adimula, A. (1989): Variation in raindrop size distribution and specific attenuation in a tropical environment, URSI Comm.. F Symp., La Londe-les Maures, France. PP 8.1.1 – 8.1.4.
- Ajayi, G. O. and Oslen, R. L. (1985): Modelling of a tropical raindrop size distribution for microwave and millimetre wave applications. Radio Sci. Vol. 20, NO. 2. PP193 – 202.
- Andreas Schiffler (1996) : Magneto-ionic Theory and Appleton-Hartree Equation
- Battan, L. J. (1973): Radar observation of the atmosphere. Uni. Of Chicago Press, Chicago IL.
- Campbell, I .M. (1997): Energy and the Atmosphere; A Physical and Chemical Approach. New York, John Willey and Sons Limited. PP 19 – 22, 42 – 57.
- Constantine, A. Balanis (1982): Antena Theory; Analysis and Design. John Willey and Sons, Toronto. PP 48 – 53
- Hall, M. P. M. and Barclay, L. W. (1991): Radio wave propagation. Peter Peregrinus, London. PP 75 – 80, 175 –177, 184 – 187.
- International Telecommunication Union Radio, (2000); Propagation Data and Prediction Methods required for the design of earth-space Telecommunication Systems. PP 5 – 6.
- Joss, J., Thams, J. C. and Waldvogel, A. (1986): The variation of raindrop size distributions at Lorcano, Switzerland. Proc. Int. Conf. on Cloud Physics, Toronto, Canada. PP 369 – 373.

- Law, J. O. and Parson, D. A. (1943): the relation of raindrop sizes to intensity. Transaction of American Geophys. Union. Vol. 24, PP 432 – 460.
- Maral, G. and Bousquet, M. (1998): satellite communication systems. Great Britain. PP 15 – 59.
- Marshall, J. S. and Palmer W. M. K. (1948): The distribution of raindrops with size. Journal of Meterology, Vol. 5 PP 165 – 166
- Nelson, A. R. and Gakhale, N. R. (1972): Oscillation frequencies of freely suspended water drops. Journal of Geophys. Res. Vol. 77, PP 724 – 2727.
- Richard, P. Wayne (1993): Chemistry of Atmospheres. Claredon Press Oxford, New York PP 36 –47.
- Ray, P. S. (1972): Broadband Complex refractive indices of ice and water. Applied Optics, Vol. II, No. 8, PP 1836-1844.
- Radio Society of Great Britain (1994): Microwave Handbook. Britain, Vol. 1 PP 4.18 – 4.37.
- Roger, G. Barry and Richard, J. Chorley (1982): Atmospheric, Weather and Climate. Richard Clay Limited, New York, PP 1.
- Saunders, J. (1975): Rain attenuation of millimetre waves at wavelength 5.77, 3.3 and 2mm. IEEE Transc. on Ant. and propagations. Vol. AP-23, No. 2, PP 213-220.
- Sazonov, D. M. (1990): Microwave circuit and antennas. Mir publisher, Moscow, PP 227, 435-446.

Smith, K.E. and S. Weintraub (1953): the constants in the equation for atmospheric refractive index at radio frequencies. Proc IRE. Vol. 44 PP 1035-1037.

Telsat Communication (1996): A Technical Look at Transmitting Stations, New Zealand PP1-13

Timothy, Pratt and Charles, W Bostian (1986): Satellite communications, New York, Willey and Sons Limited. PP 22-30, 334-337.

United Nations Educational Scientific and Cultural Organization. (1996): Handbook on radio propagation related to satellite communication in tropic and subtropical countries, PP 201-211, 225-229.

Ugai and Akimoto (Private Correspondence).